MARINE SCIENCE AND TECHNOLOGY BULLETIN

Volume 8 - Issue 1 - YEAR 2019

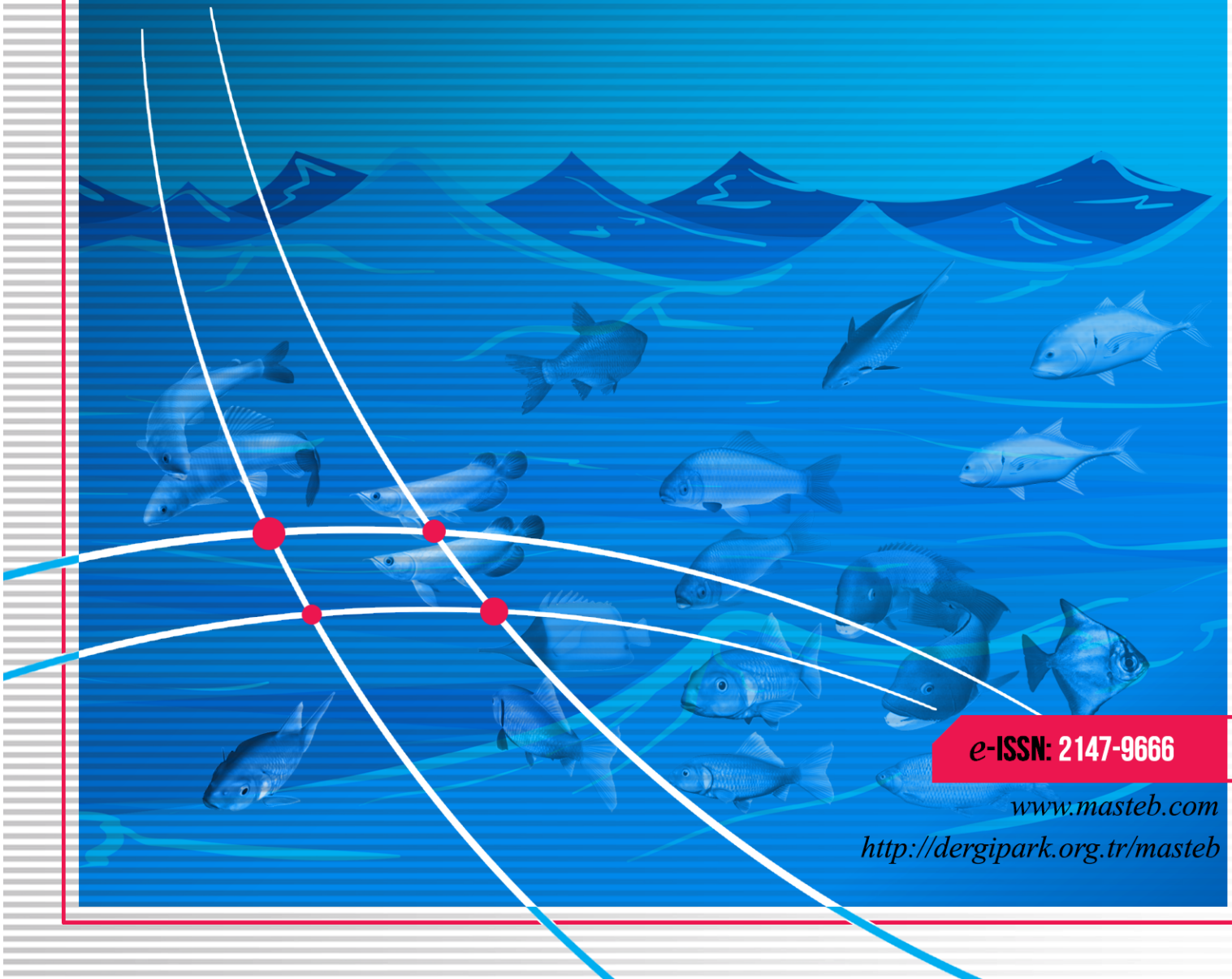

e-ISSN: 2147-9666

www.masteb.com

http://dergipark.org.tr/masteb

MARINE SCIENCE AND TECHNOLOGY BULLETIN

VOLUME: 8 • ISSUE: 1 • JUNE 2019

AUTHOR GUIDELINES

Manuscripts must be submitted to the journal in electronic version only via online submission system at http://dergipark.org.tr/masteb.

Types of Paper

- Original research papers; review articles; short communications; letters to the Editor; book reviews.
- *Original research papers*; original full-length research papers which have not been published previously and should not exceed 7500 words or 25 manuscript pages (including tables and illustrations)
- *Review articles*; on topical subjects and up to 10,000 words or 25 manuscript pages (including tables and figures)
- *Short communications*; describing work that may be of a preliminary nature (preferably no more than 3000 or 10 manuscript pages including tables and figures).
- *Letters to the Editor*; should be included on matters of topical interest and not exceeding 2000 words or 10 manuscript pages including tables and figures)
- *Book reviews* are also published.

Page charges

This journal has no page charges.

Preparation of Manuscripts

Papers must be written in English. Prepare your text using a word-processing software and save in *".doc"* or *".docx"* formats. Manuscripts must be structured in the following order;

- Title page
  - Title
  - Author names and affiliations
  - Corresponding author's e-mail, Telephone, Fax
  - The number of figures
  - The number of tables
- Main text
  - Abstract
  - Keywords
  - Introduction
  - Material and Methods
  - Results
  - Discussion
  - Conclusion
  - Acknowledgement (if required)
  - Conflict of Interest
  - References
- Table(s) with caption(s) (on appropriate location in the text)
- Figure(s) with caption(s) (on appropriate location in the text)
- And appendices (if any)

Use a 12-point font (Times Roman preferred), including the references, table headings and figure captions, double-spaced and with 25 mm margins on one side of A4 size paper throughout the manuscript. Use 25 mm margins on all sides. The text should be in single-column format. In particular, do not use to hyphenate words. The names of genera and species should be given in *italics* and, when first mentioned in the text, should be followed by the authority. Authors should consult a recent issue of the journal for style if possible.

Title Page

The title page should be included;

- Concise and informative title. Avoid abbreviations and formulae
- The first name(s) and surname(s) of the author(s) (The corresponding author should be identified with an asterisk and footnote. All other footnotes (Author(s) affiliation address(es)) should be identified with superscript numbers)
- Author(s) affiliation address(es) (followed by department, institution, city with postcode, and country) of the each author(s))
- The e-mail address, phone number, fax number of the corresponding author
- The number of figures
- The number of tables

Main Text

- Abstract (should not exceed 500 words. References and abbreviations should be avoided)
- Keywords (provide a maximum of 6 keywords)
- Articles must be structured in the conventional format such as Introduction, Material and Methods, Results, Discussion, Conclusion, Acknowledgments, Conflict of Interest, and References.
- Each page must be numbered, and lines must be consecutively numbered from the start to the end of the manuscript.
- Do not justify on the right-hand margin.
- The first line of each paragraph must be indent. Do not put a blank line between paragraphs.
- The first mention in the text of any taxon must be followed by its authority including the year.
- Use italics for emphasis.
- Use only SI (international system) units.

Acknowledgement

Keep these to the absolute minimum and placed before the reference section.

References

Citation in text;

Please ensure that each reference cited in the text is also presented in the reference list. Cite literature in the text in chronological, followed by alphabetical order like these examples "(Mutlu et al., 2012; Biswas et al., 2016; Yanık and Aslan, 2018)". If the cited reference is the subject of a sentence, only the date should be given in parentheses. Formatted like this examples: "Sönmez (2017)".

- Single author: the author's name and the year of publication;
- Two authors: both authors' names and the year of publication;
- Three or more authors: first author's name followed by "et al." and the year of publication (all authors are to be listed at first citation)

Citation in the reference list;

References should be listed first alphabetically and then further sorted chronologically at the end of the article. More than one reference from the same author(s) in the same year must be identified by the letters a, b, c, etc. placed after the year of publication.

The citation of articles, books, multi-author books and articles published online should conform to the following examples:

Article:

Yamasaki, J., Miyata, H. & Kanai, A. (2005). Finite-difference simulation of green water impact on fixed and moving bodies. *Journal of Marine Science and Technology*, ***10***(1): 1-10.

Yanık, T. & Aslan, İ. (2018). Impact of global warming on aquatic animals. *Pakistan Journal of Zoology*, ***50***(1): 353-363.

Sönmez, A.Y., Kale, S., Özdemir, R.C. & Kadak, A.E. (2018). An adaptive neuro-fuzzy inference system (ANFIS) to predict of cadmium (Cd) concentration in the Filyos River, Turkey. *Turkish Journal of Fisheries and Aquatic Sciences*, ***18***(12): 1333-1343.

Book:

Brown, C., Laland, K. & Krause, J. (Eds.) (2011). Fish Cognition and Behavior. 2nd ed. Oxford, UK: Wiley-Blackwell. 472p.

Chapter:

Langston, W.J. (1990). Toxic effects of metals and the incidence of marine ecosystems, p. 102-l22. In: Furness, R.W. (Eds.), Rainbow heavy metals in the marine environment. CRC Pres., New York. 256p.

Vassallo, A.I. & Mora, M.S. (2007). Interspecific scaling and ontogenetic growth patterns of the skull in living and fossil ctenomyid and octodontid rodents (Caviomorpha: Octodontoidea). In: Kelt, D.A., Lessa, E., Salazar-Bravo, J.A., Patton, J.L. (Eds.), The Quintessential Naturalist: Honoring the Life and Legacy of Oliver P. Pearson. 1st ed. Berkeley, CA, USA: University of California Press, pp. 945-968.

Thesis:

Sönmez, A.Y. (2011). Karasu ırmağında ağır metal kirliliğinin belirlenmesi ve bulanık mantıkla değerlendirilmesi. Ph.D. Thesis. Kastamonu University, Kastamonu, Turkey.

Conference Proceedings:

Notev, E. & Uzunova, S. (2008). A new biological method for water quality improvement. *Proceedings of the 2nd Conference of Small and Decentralized Water and Wastewater Treatment Plants*, Greece, pp. 487-492.

Institution Publication:

FAO. (2016). *The State of World Fisheries and Aquaculture: Contributing to food security and nutrition for all*. Rome. 200 pp.

Report:

FAO. (2018). *Report of the ninth session of the Sub-Committee on Aquaculture*. FAO Fisheries and Aquaculture Report No. 1188. Rome, Italy.

Internet Source:

Froese, R. & Pauly, D. (Eds.) (2018). FishBase. World Wide Web electronic publication. Retrieved in January 11, 2018 from http://www.fishbase.org.

Table(s)

Tables, numbered in Arabic, should be on separate pages with a short descriptive title at the top. Place footnotes to tables below the table body and indicate them with superscript lowercase letters (or asterisks for significance values and other statistical data). Avoid vertical rules. The data presented in tables do not duplicate results described elsewhere in the article.

Figure(s)

All illustrations should be labelled 'Figure' and numbered in consecutive Arabic numbers, Figure 1, Figure 2 etc. m the text. If panels of a figure are labelled (a, b, etc.) use the same case when referring to these panels in the text. Drawings reproduced with a high quality laser printer are preferred. Photographs, 1f used, should be of good contrast and printed on glossy paper. Figures, which are recommended for electronic formats such as PNG, JPEG. TIFF (min. 300 dpi) should be also arranged m available dimensions. All figures or tables should be presented in the body of the text. Use the Times New Roman font for all figures and tables. Font sizes size should be from 9 to 11 points.

Download Copyright Form

SCOPE

The *Marine Science and Technology Bulletin* is an international, double blind peer-reviewed and open access journal publishing high quality papers that original research articles, short communications, technical notes, reports and reviews for scientists engaged in all aspects of marine sciences and technology, fisheries and aquatic sciences both fresh water and marine, and food processing technologies.

Research areas include (but not limited):

Marine Sciences
Marine Technology,
Fisheries and Aquatic Sciences,
Environmental Science and Technology,
Oceanography,
Limnology,
Marine Biology,
Marine Ecology,
Marine Engineering,
Ocean Engineering,
Offshore and Underwater Technology,
Biology,
Ecology,
Biogeography,
Aquaculture,
Fish Nutrition,
Disease and Treatment,
Fisheries Technology,
Food Processing,
Chemistry,
Microbiology,
Algal Biotechnology,
Maritime,
Marine Affair,
Naval Architecture,
Marine and Freshwater Pollution,
Management and Economics,
Unmanned Surface/Underwater Vehicles,
Remote Sensing,
Information Technologies,
Computational Mechanics,
Artificial Intelligence,
Fuzzy Logic,
Image Processing Technology,
Climate Change,
Protection of Organisms Living in Marine, Brackish and Freshwater Habitats.

Online Manuscript Submission

Authors are requested to submit manuscripts via the journal's online submission system following the Instructions for Authors.

Peer Review Process

All submitted manuscripts are subject to initial appraisal by the Co-Editors, and, if found suitable for further consideration, enter peer review by independent, anonymous expert referees. All peer review is double-blind.

Publication Frequency

The journal includes original scientific articles on a variety of different subjects in English and is published two times a year in June and December.

Publication Fees

No submission or publication charges are collected. All authors and readers have free access to all papers.

REVIEW PROCESS

Double-Blind Review and Evaluation Process

Double-Blind Review is a method applied for publishing scientific publications with the highest quality. This method forms the basis of an objective evaluation of scientific studies and is preferred by many scientific journals.

The views of referees have a decisive place in the publication quality of Marine Science and Technology Bulletin.

Marine Science and Technology Bulletin uses the double-blind review method, which means that both the reviewer and author identities are concealed from the reviewers, and vice versa, throughout the review process, in the evaluation process of all studies. For this reason, the authors are asked to erase their names while uploading the articles to the system.

All the studies sent to Marine Science and Technology Bulletin are evaluated by double-blind review method according to the following steps.

1. Initial Evaluation Process

The studies submitted to *Marine Science and Technology Bulletin* are first evaluated by the editor. At this stage, studies that are not in line with the aim and scope of the journal, are weak in terms of language and narrative rules in English contain scientifically critical mistakes, are not original worthy and cannot meet publication policies are rejected. Authors of rejected studies will be notified within one month at the latest from the date of submission. Eligible studies are sent to the field editor to which the study is relevant for pre-evaluation.

2. Pre-Evaluation Process

In the pre-evaluation process, the field editors examine the studies, introduction and literature, methods, findings, results, evaluation and discussion sections in detail in terms of journal publication policies, scope and authenticity of study. Study which is not suitable as a result of this examination is returned to the author with the field editor's evaluation report within four weeks at the latest. The studies which are suitable for the journal are passed to the referee process.

3. Referee Process

The studies are sent to the referees according to their content and the expertise of the referees. The field editor examining the study may propose at least two referees from the pool of Marine Science and Technology Bulletin Advisory Board or referee pool according to their field of expertise or may propose a new referee appropriate to the field of study.

The editors evaluate the referee's suggestions coming from the field editor and the studies are submitted to the referees. Referees are obliged to guarantee that they will not share any process or document about the study they are evaluating.

4. Referee Evaluation Process

The period given to the referee for the evaluation process is 15 days. Proposals for corrections from referees or editors must be completed by the authors within 1 month according to the "correction instruction".

Referees can decide on the suitability of the study by reviewing the corrections and may also request multiple corrections if necessary.

Referee Reports

Referee evaluations are based in general on the originality of the studies, the method used, and the conformity with the ethical rules, the consistent presentation of the findings and results, and the examination of the literature.

This review is based on the following elements:

1. Introduction and Literature: The evaluation report contains the presentation and purpose of the problem addressed in the study, the importance of the topic, the scope of the relevant literature, the timeliness and the originality of the study.

2. Methodology: The evaluation report includes information on the suitability of the method used, the choice and characteristics of the research group, validity and reliability, as well as on the data collection and analysis process.

3. Findings: The evaluation report includes opinions on the presentation of the findings obtained in the frame of the method, the correctness of the analysis methods, the aims of the research and the consistency of the findings, the presentation of the required tables, figures and images and the conceptual evaluation of the tests used.

4. Evaluation and discussion: The evaluation report includes the opinion on the subject based on findings, relevance to research questions and hypotheses, generalizability and applicability.

5. Conclusion and suggestions: The evaluation report contains the opinion on the contributions to the literature, future studies and recommendations for the applications in the area.

6. Style and narration: The evaluation report includes compatibility of the headline with the content, appropriate use of English in the study, refers and references in accordance with the language of the study and APA rules.

7. Overall evaluation: The evaluation report contains opinion on the authenticity of the study as a whole, its contribution to the educational literature and the applications in the area.

The journal considers that scientists should avoid research which kills or damages any species of fish which, using IUCN criteria, is regarded as threatened or is listed as such in a Red Data Book appropriate for the geographic area concerned. In accordance with this view, papers based on such research will not be accepted by the Journal, unless the work had clear conservation objectives.

Plagiarism Detection

In agreement with publishing policies of *Marine Science and Technology Bulletin*, plagiarism check is required for each study that has undergone the "Review Process". The *Turnitin* plagiarism checker software is used for plagiarism detection.

Proofs

Proof documents will be sent to the corresponding authors via online submission system. Proofs should be checked immediately and responses should be returned back within 15 working days. It is the responsibility of the authors to check carefully the proofs. No changes will be allowed at this stage.

DISCLAIMER

This journal is available online at DergiPark Open Journal System. Visit http://dergipark.org.tr/masteb & http://www.masteb.com to search the articles and register for table of contents e-mail alerts.

LICENSE

INDEXING

Marine Science and Technology Bulletin is indexed by "*CAB Abstracts, CAB Direct, Index Copernicus, Directory of Research Journals Indexing (DRJI), CiteFactor, Eurasian Scientific Journal Index, Scientific Journal Impact Factor (SJIF), COSMOS IMPACT FACTOR, Scientific Indexing Services (SIS), ASOS INDEX, General Impact Factor, International Innovative Journal of Impact Factor (IIJIF), Genamics JournalSeek, International Institute For Research Impact Factor Journals (IFJ), ResearchBib, ACADEMIC JOURNAL INDEX (AJI), Bielefeld Academic Search Engine (BASE), International Institute of Organized Research (I2OR), AcademicKeys, Root Indexing, Journal Factor, International Citation Indexing (ICI), Paperity, Google Scholar*"

MARINE SCIENCE AND TECHNOLOGY BULLETIN VOLUME 8 • ISSUE 1 • JUNE 2019

TABLE OF CONTENTS

RESEARCH ARTICLES

Mar. Sci. Tech. Bull. (2019) 8(1): 1–9

e–ISSN: 2147–9666

info@masteb.com

http://dergipark.gov.tr/masteb

http://www.masteb.com/

DOI: 10.33714/masteb.486678

RESEARCH ARTICLE

An empirical study of R applications for data analysis in marine geology

Polina Lemenkova[1*]

[1] *Ocean University of China, College of Marine Geoscience, Qingdao, China*

ARTICLE INFO

Article History:

Received: 22.11.2018

Received in revised form: 27.02.2019

Accepted: 08.03.2019

Available online: 15.03.2019

Keywords:

R programming

Statistical analysis

Mariana Trench

Bathymetry

ABSTRACT

The study focuses on the application of R programming language towards marine geological research with a case study of Mariana Trench. Due to its logical and straightforward syntax, multi–functional standard libraries, R is especially attractive to the geologists for the scientific computing. Using R libraries, the unevenness of various factors affecting Mariana Trench geomorphic structure has been studied. These include sediment thickness, slope steepness, angle aspect, depth at the basement and magmatism of the nearby areas. Methods includes using following R libraries: {ggplot2} for regression analysis, Kernel density curves, compositional charts; {ggalt} for Dumbbell charts for data comparison by tectonic plates, ranking dot plots for correlation analysis; {vcd} for mosaic plots, silhouette plots for compositional similarities among the bathymetric profiles, association plots; {car} for ANOVA. Bathymetric GIS data processing was done in QGIS and LaTeX. The innovativeness of the work consists in the multi–disciplinary approach combining GIS analysis and statistical methods of R which contributes towards studies of ocean trenches, aimed at geospatial analysis of big data.

Please cite this paper as follows:

Lemenkova, P. (2019). An empirical study of R applications for data analysis in marine geology. *Marine Science and Technology Bulletin*, 8(1): 1–9.

Introduction

The Mariana Trench is the deepest point of the Earth located in the western part of the Pacific Ocean, eastwards to Philippine islands and China (Figure 1). It crosses four tectonic plates: Caroline, Pacific, Philippine Sea and Mariana. The Mariana Trench has unique features in its geomorphology, complex geological and lithological structures. The geologic features of the Mariana Trench are briefly discussed below.

Geographic Location

Mariana Trench belongs to the deepest trenches of the Earth, with maximal depths above 9–11 km, all of which are located in the western half of the Pacific Ocean.

* Corresponding author

E-mail address: lemenkovapolina@stu.ouc.edu.cn; pauline.lemenkova@gmail.com (P.Lemenkova)

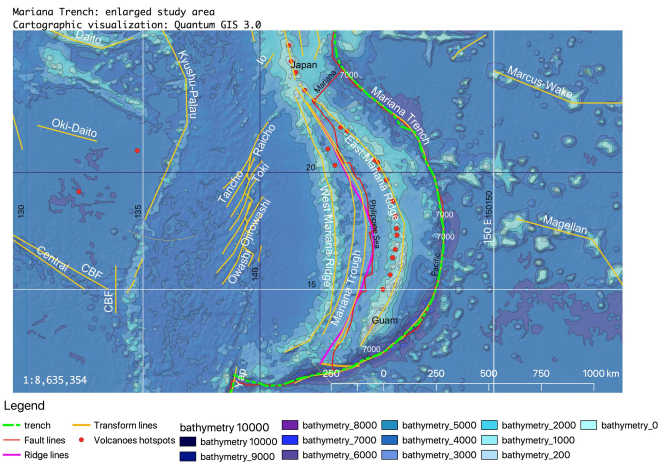

Figure 1. Study area: Mariana Trench (Cartography was created by Quantum GIS (QGIS) software)

The geographic location of the edge of the Mariana Trench along the coasts of the continents or island arcs is explained mainly by the subduction of oceanic tectonic plates at the boundaries of their collision with Mariana, Pacific, Philippine, Caroline tectonic plates (Ishibashi et al., 2015).

The seabed structure of the Mariana Trench is composed in the following way from top to bottom: a sedimentary cover, a basalt of the leitic composition, a complex of parallel dykes of diabases, an isotropic gabbro, a banded gabbro–ultrabasic complex lying on the mantle ultrabasites (Butuzova, 2003). There are differences in the velocity of the longitudinal seismic waves in the geological layers of the Mariana Trench structure: water and sedimentary layer have a speed of 3.5 – 6.2 km/s, basaltic layer has a speed of 6.5–7.0 km/s. The layer of gabbro and banded gabbro are located beneath. The boundary of the crust–mantle is made up by a sharp increase in the velocities from 7 to 8 km/s (the boundary of the Mohorovicic). The upper mantle is the region with the velocities of 8.0–8.2 km/s (Garfunkel et al., 1986). Analogues of the oceanic crust on the ground are ophiolites (Figure 2).

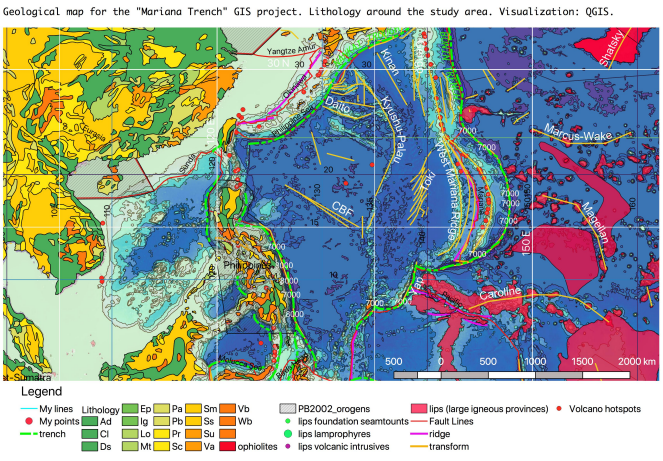

Figure 2. Lithology of the Mariana Trench area, Pacific Ocean (This map was created by QGIS software)

The average thickness of the crust of this type under the platforms is about 40 km (Gurevich, 1998). The regions with bark continental type in the ocean are fragments of continental mass formed as a result of the formation of the modern ocean floor causing migration and slow movement of the trench (Husson, 2012).

Sedimentation and Lithology

The lithological structure and sediment thickness are among the other factors affecting Mariana Trench formation. Relatively few other trenches, when compared to Mariana Trench, are also formed on the boundaries of the tectonic plates, but usually at a greater distance from the continents in the rift zones. Therefore, the sedimentation processes within Marina Trench are deeply impacted by the location near the rift zones that are mainly associated with the formation of the underwater mountain ranges and spreading. Their expansion in the sides of the neighbouring lithospheric plates is a result of the rise towards Mariana Trench.

Geometrically, the transversed faults are formed sub–orthogonal to major normal faults. They are created as local shortening structures with uneven depths above lateral and oblique extensional ramps. This creates excellent conditions for sedimentation accumulation of the outflow of the substance coming from the upper layer of the earth's mantle. According to available geophysical data (Dubinin and Ushakov, 2001), the oceanic crust of the tectonic plates surrounding Mariana Trench is composed by a number of layers. Therefore, the impact of the sediment subduction on the trench dynamics is relatively high, which is highlighted by Horleston and Helffrich (2012).

Geomorphology

The adjusting continental slopes are high, reaching up to several thousand meters and inclining to 3–6° (in the south–western part of the trench up to 30–40 °), the upper boundary of which coincides with the edges of the shelf (depths of 150–200 m). Slopes of the passive margins are strongly complicated by the terraces, ledges, marginal plateaus and canyons. Slopes of the margins are steeper, reaching can 5–7 km in height. The geomorphic structure of the Mariana Trench is complicated by the longitudinal ridges, steps, large landslide bodies and ledges. At the base of the continental slope of passive margins formed by the adjacent tectonic plates, Philippine Sea, Pacific and Caroline on the south–west, continental foot forms accumulative body. In turn, it is formed by the merged cones of the removal and plumes of the suspension flows and submarine landslides with abyssal sedimentation.

Submarine margins of continents or transition zones depend on the features of the relief and geology. According to them, they are divided into two types: the passive ones and the active ones. The first ones include the shelf that is mainland bank, the slope and the mainland foot. Having complicated relief structure with marginal seas, island arcs and deep–sea gutters, Mariana Trench belongs to the active type of trench. Due to the geodynamic reasons, Mariana Trench motion, migration and upper plate deformation can be described as the result of the response to the mantle flow and the imbalance between the forces exerted by the lower and upper continental plates at the plate interface.

Bathymetry

The deepest point of the Mariana Trench, the Challenger Deep, is located in the south–west of the trench with maximal depth of 10,984±25 m (95%) at 11.329903°N / 142.199305°E (Gardner et al., 2014). North–western Pacific Ocean is especially characteristic for the vast areas of the bottom of the basins occupied by depressions deeper 6000 m with a special case of Mariana Trench. Despite the extreme bathymetric values of the Mariana Trench at Challenger Deep, its structure has the following pattern: a major total area is being occupied by the abyssal depths (3–6 km), while the extreme depths exceeding 6 km, are smaller in comparison to the previous areas (Uyeda and Kanamori, 1979).

The abyssal make up relatively small part of the total area of the Mariana Trench, while the second ones cover about two thirds of the whole. Depths of more than 6000 m are confined mainly to the deepest part of the trench located in the south–western part of Mariana, although individual depressions to depths of 6–7 km, rarely up to 7.5 km, occur in the central part of the basins along the trench (Morgan, 1974). The typical depths of the ocean floor of the Mariana Trench are 4000–5000 m where mid–ocean ridges and deep–sea basins formed by numerous mountains and depressions are located. The general form of the bathymetric structure of the Mariana Trench is inclined toward the margin plate being connected with the ocean basic zone. It has high and steep island or continental slopes and more low and gentle slopes from the south–eastern side. The main area of the seafloor of the trench has prevailing depths of more than 3000 m, a seabed being the most ancient parts of the ocean floor formed in the late Jurassic.

Material and Methods

In this paper, a combination of various approaches has been used in the methodology workflow. Several R packages were applied for importing and manipulating geospatial data, combined with statistical machine learning. Various algorithms of data visualization were tested to facilitate spatial analysis using data from the GIS project: geology, tectonics, bathymetry, sedimentation, etc. The technical tools supporting this research include GIS, statistical methods and approaches made by R programming (e.g. Warner et al., 2008; Oliphant, 2007; Roberts et al., 2010). Recently developed powerful technologies provided by R, Matlab or Octava software, enable to perform precise computations and statistical analysis of big data as well as to create data frames in geosciences. Among others, a python language has become increasingly popular (Lin, 2008, Marta–Almeida et al., 2011). Nowadays, the machine learning and data mining for the oceanological research are among the most important technical goals. Using R programming (R Core Team, 2018) based machine learning algorithms ensure the preciseness and objectiveness of the big data set processing, which is always the case for oceanographic research.

However, a combination of the statistical methods with GIS dramatically increases the effectiveness of the research due to the embedded machine learning algorithms that enable to process big data frames dividing them into compatible data sets for statistical analysis. For instance, we can select several attribute tables specifically for magmatism of the nearby areas to analyse the possibilities of the earthquakes, or to focus on the bathymetric properties and distribution of various depth values across the selected profiles, etc. Special packages of the R programming include mathematical algorithms and a range of codes specially designed for statistical analysis, as demonstrated below. In the scope of current research, a functionality of R language has been tested. Indeed, it proved to be as an effective tool for studying distribution of the environmental factors affecting the structure of the trench, as well as bathymetric clusters grouped by the similarity of the geomorphic properties at the seafloor basement of the Mariana Trench.

The methodological workflow of the current work includes following steps:

i. Bathymetric GIS Data Processing in QGIS and LaTeX;
ii. Statistical analysis on data distribution: Kernel density and regression analysis with 3 approaches: linear, locally estimated scatterplot smoothing (loess) and general linear methods;
iii. Dumbbell charts for data pairwise comparison by tectonic plates;
iv. Ranking dot plots for correlation between the determinants (trench slope steepness in tg° angle by bathymetric profiles, igneous volcanic areas, depth);
v. Compositional "waffle" charts showing variation of the aspect and steepness classes of the trench basement angle, by 25 bathymetric profiles;
vi. Mosaic plots with standardised residuals to assess data distribution and silhouette plot for compositional similarities among the bathymetric profiles;
vii. Association plots with statistical Pearson residuals to analyse model fitness at each observation data set for generalized linear models;
viii. ANOVA (Analysis of Variance) to assess hypothesis testing.

Bathymetric GIS Data Processing

The digitizing of the 25 bathymetric profiles across the trench has been performed in QGIS.

The length of each profile was taken at 1000 km, and the distance between every pair was 100 km. The coordinates were saved in a table with three columns: elevations, latitude and longitude. After a square of the area was crossed by the profiles, the .csv table was imported for processing in LaTeX. The visualization of the 25 profiles grouped by three and four has been performed in LaTeX (Figure 3). Technically, the following script was used:

```
\begin{filecontents*}{MyTab18.csv}
ELEV,y2,x2
145.528246366,47.0433461696,–7800 # bathymetric data here in 3
    columns
\end{filecontents*}
\begin{tikzpicture}
```

\begin{axis}[grid=major,minor x tick num=10,minor y tick num=10,colorbar sampled line,colormap name=bluered,title={Mariana Trench. Bathymetric Profiles Nr.16,17,18},ylabel={Depth (m)},legend entries={Profile18,Profile17,Profile16,},scaled ticks=false,yticklabel style={

/pgf/number format/fixed,

/pgf/number format/fixed zerofill,}]

\addplot+ [scatter,only marks,mark=Mercedes star flipped,colormap name=bluered,] table [x=x, y=d, col sep=comma] {MyTab16.csv};

\addplot+ [scatter, colorbar sampled line,only marks,mark=asterisk,colormap name=bluered,] table [x=long, y=d, col sep=comma] {MyTab17.csv};

\addplot+ [scatter, colorbar sampled line,only marks,mark=10-pointed star,colormap name=bluered,] table [x=y2,y=ELEV, col sep=comma] {MyTab18.csv};

\end{axis} \end{tikzpicture}

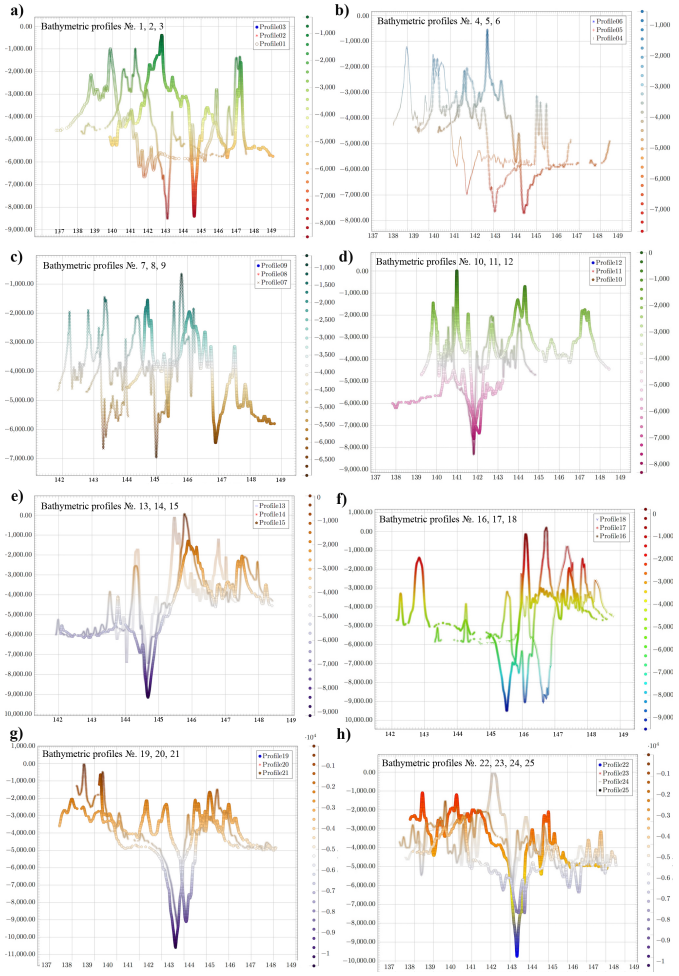

Figure 3. 25 cross-section bathymetric profiles of Mariana Trench. a) profiles 1, 2, 3; b) profiles 4, 5, 6; c) profiles 7, 8, 9; d) profiles 10, 11, 12; e) profiles 13, 14, 15; f) profiles 14, 15, 16; g) profiles 19, 20, 21; h) profiles 22, 23, 24, 25 (Plots were created in LaTeX)

Regression Analysis of Data Distribution: R library {ggplot2}

Hence, depending on the structure and size of the availability data frame, the methodological approaches of the assessment of data distribution may change. However, the most essential statistical analysis of the ocean research would start by the question of data distribution. Computing and plotting Kernel distribution curves, box plots, regression lines (probability of bathymetric data across profiles), quantile statistics, empirical distribution density function and other methods can be distinguished as the most useful for initial data processing.

The principle of the regression analysis is based on the analysis of the probability of the data values according to their actual distribution. A regression analysis represents outlying depths observations by each bathymetric profile, as shown on the example of three profiles in Figure 4. This methodology utilizes the relation between two or more quantitative depth variables so that one variable can be predicted from another. Thus, one can estimate the probability that the depth values will be located in this or that interval of values profile by profile according to the machine-based algorithm of the probability of their distribution. Kernel density distribution shows the majority of the depths of the trench between 3000 and 6000 m. The graph has been made as a combined plot (Figure 5) enabling to compare the overlapping and maximal aptitude of the density curves for both the profiles and depth data distribution by four tectonic plates.

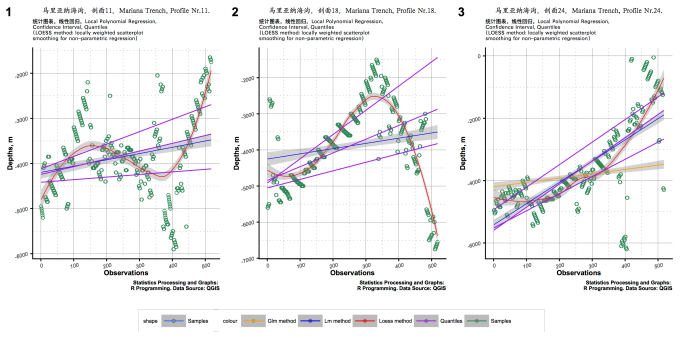

Figure 4. Regression analysis for selected profiles, R programming

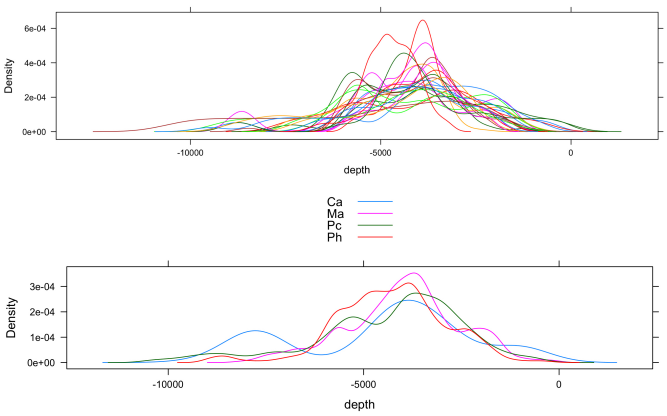

Figure 5. Kernel density estimation for 25 bathymetric profiles (Graph was created by using R)

Dumbbell Charts for Data Pairwise Comparison by Tectonic Plates

Because Mariana Trench crosses four tectonic plates (Mariana, Caroline, Philippine and Pacific) the comparative testing of the values distribution by adjacent tectonic plates has been completed through the Dumbbell chart plotting. Dumbbell chart is a visualization aimed to give an insight of how the margin tectonic plates constitute to the Mariana Trench pairwise. It is one of the new statistical methods which was initially widely used in biosciences, yet it can be applied to spatial analyses when it is necessary to take pairwise comparison of the data distribution from any thematic layer. Plotting has been carried out by calling R libraries {ggplot2} and {ggalt}. Dumbbell chart demonstrates (Figure 6) pairwise distribution of the bathymetric points constituting the continental plates, to show the composition of the sedimentary coverage by four tectonic plates.

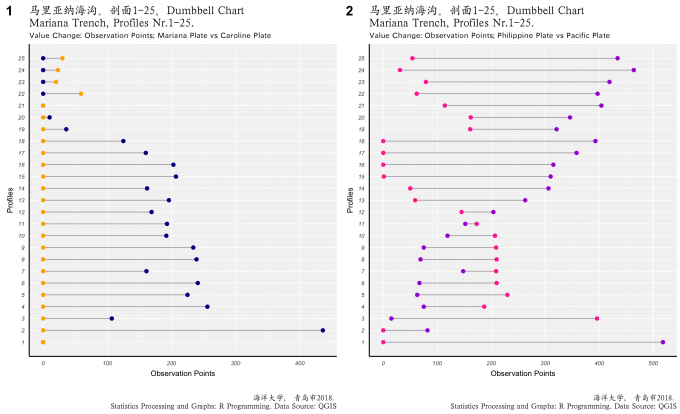

Figure 6. Dumbbell diagrams for pairwise comparison of the tectonic plates

The Y axis shows the profiles and the X axis – the number of observation points crossing to the given tectonic plate. In this case the comparison was given by pairs Philippine sea and Pacific plate, and Mariana and Caroline Plates, respectively. Although a complete comparison of all the environmental determinants has not yet been given (in the scope of this research only bathymetric points were plotted for the Dumbbell chart), a certain insight of the tectonic structure of the Mariana Trench contributes to understanding of the congruence of the ocean floor by four plates.

Ranking Dot Plots by Data Grouping

Pairwise correlation was visualized by the ranking dot plots, which is an effective tool to perform data grouping by variables: tectonic plates. Plotting distribution of the observation points by igneous volcanic areas aimed at visualizing areas affected by the magmatism. Large igneous volcanic areas contribute towards localization of possible earthquake zones. Thus, as can be drawn from the plot (Figure 7), the volcanic areas increase along Mariana Trench south–westwards.

Alike to the volcanic areas plotting, the variation of the steepness slope was performed using ranking dot plot: the bathymetric profiles with the steepest angles across the trench are located in the north–eastern part with a slight decrease towards the south–west. To calculate tgº angle of the profiles, a standardized formula was used, that is a relation of the maximal depth by profiles divided by the width of the corresponding bathymetric profile. The crucial points (Figure 7) were selected using library{ggalt} by calling following R code:

```
crucial_igneous<MDF[MDF$igneous_volc > 50 &
    MDF$igneous_volc <= 300 & MDF$profile > 5 &
    MDF$profile <= 25, ]

crucial_angles <- MDF[MDF$tg_angle > 0.00 & MDF$tg_angle
    <= 0.075 & MDF$profile > 5 & MDF$profile <= 22, ]
```

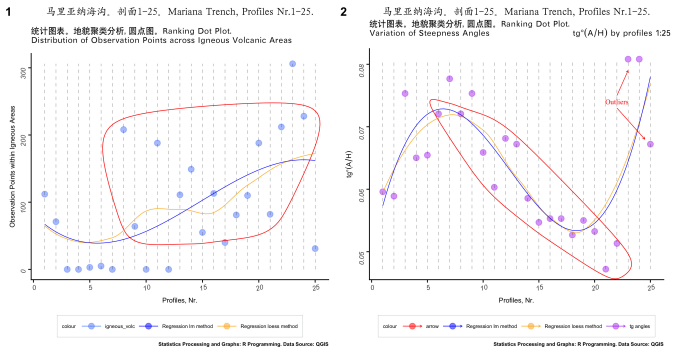

Figure 7. Ranking dot plots by data grouping

The distribution of angle steepness values across the trench have been shaped by the components of the igneous volcanic areas near the profiles, as understood from the Figure 7: profiles # 20, 22, 24, 8 and 11 with notable amount of igneous volcanic observation points (over 180) correlate with steepness angle.

Compositional Charts of the Determinants Variations

The constitution of the system composition has been visualized by the categorical plotting. One of the methods enabling categorical plotting is presented by compositional charts, sometimes referred to as "waffle charts". The core idea of this method is to demonstrate the division of the whole system by parts in percentage. Several R libraries can be used to perform technically compositional plotting, of which the {ggplot2} has been selected as the most effective: it enables to control the appearance of the plot by adjusting details (colors, font size and types, plotting two graphs together, etc).

The compositional chart is aimed to compare the distribution of the data across the study area, as well as the composition of the aspect class and slope angle for the Mariana Trench. As can be drawn from the chart (Figure 8), the category "very steep slope" is the dominant among all other geomorphological types of the slope degree of the Mariana Trench. Likewise, north and south–west aspect of the slope direction perfectly describes the geometry of the northern and southern part of the trench, respectively.

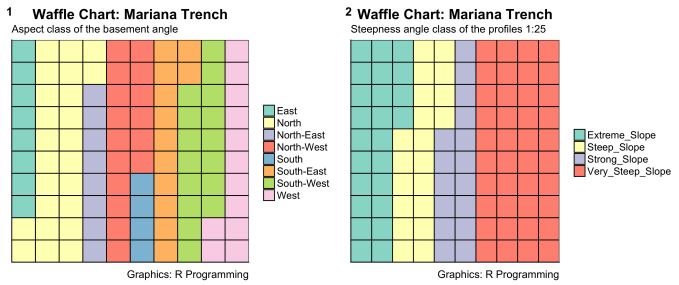

Figure 8. Compositional chart of geometric properties of the Mariana Trench

Mosaic and Silhouette Plots of the Observation Data by Tectonic Plates

Mosaic chart aims at categorical comparison of the geomorphological features of the trench by four tectonic plates. Visualizing mosaic plot (Figure 9) is a statistical method that involves a subdivision of a rectangular tile into the areas that represent the conditional relative frequency for a cell in the contingency table.

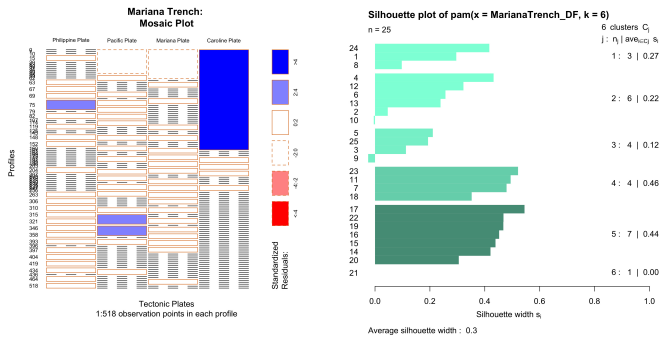

Figure 9. Mosaic plot and silhouette plots for categorical values of the environmental determinants

The algorithms and approaches used in mosaic plotting vary slightly. Upon examination of possible packages, the R library{vcd} was selected for this research. Using {vcd} library, each tile is colored to show the deviation from the expected frequency (residuals) from a Pearson X^2 or likelihood ratio G^2 test. The algorithm set includes execution of the following code:

MosaicTectRes<– mosaicplot(count, main = "Mariana Trench: \nMosaic Plot", sub = "1:518 observation points in each profile", xlab = "Tectonic Plates", ylab = "Profiles", las = 1, border = "chocolate", shade = TRUE)

The convenience of the mosaic plot for the geomorphological analysis of the ocean trenches consists in its visual representation of the association between the environmental variables. Thus, it gives an overview of the data structure and enables to recognize relationships between the different environmental variables. As can be seen from the Figure 9, the independence of the Caroline tectonic plate is shown clearly. Conversely, the boxes across categories constituting Pacific and Mariana plates have similar areas. The area of the tiles, the bin size, includes the identification of the sampling data (518 observation points across 25 bathymetric profiles), giving the proportional value to the number of observations within that category.

The interpretation and validation of consistency within clusters of geomorphologic and geological variables have been tested using silhouette method (Figure 9). This technique provides a succinct graphical representation of the suitability and fitness of each from 518 observation points across 25 bathymetric profiles within the clusters. The silhouette value measured the similarity of the points derived from the thematic layers (sediment thickness, slope steepness of the trench) to the cluster by cohesion and comparing them with other clusters, and separating them from the distinct points.

Thus, lower sediment thickness area would lie within one class while a class of areas with high level of sediment level fits to another. The silhouette ranges from −1 to +1 (Figure 9), where a high value indicates that the areas of trench are well matched to their clusters and poorly matched to the neighboring ones. To achieve the sufficient and appropriate configuration of the chosen cluster plotting, the geomorphic groups were grouped by values. The silhouette was calculated with Euclidean distance metric by calling library{cluster} using following R code:

pr5 <– pam(MarianaTrench_DF, 6)

str(si <– silhouette(pr5))

plot(si, col = c("aquamarine", "aquamarine1", "aquamarine2", "aquamarine3", "aquamarine4", "aquamarine4"))

The given script plots the silhouettes, returns the values in the n–by–1 vectors.

Association Plots with Statistical Pearson Residuals

A deviation from the independence of rows and columns containing bathymetric data and environmental variables is presented in a two–dimensional contingency table of the Cohen–Friendly association plots (Figure 10).

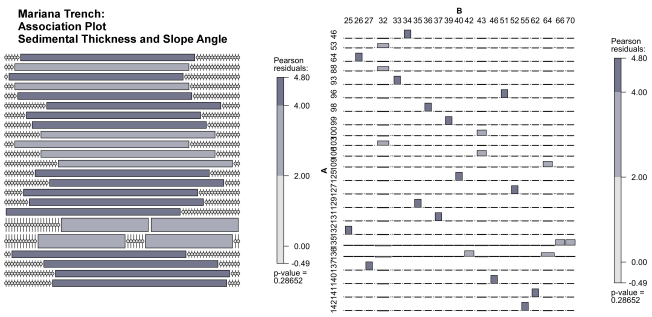

Figure 10. Association plot with statistical Pearson residuals, Mariana Trench

Extended association plot in R reveals relationships between the variables by the assoc() function in the {vcd} package. In this case, it is tectonic plates and geomorphological values (bathymetric depths, slope steepness). The Pearson's residuals on the association plot report test for the normality of residuals of the bathymetric observations. Computing Pearson's residuals enables to test whether the bathymetric samples are drawn from the identical distributions or a specified distribution, following the rules of the bathymetric structure. The

algorithm of the Pearson's computing represents the sum of the differences between the observed and expected outcome frequencies: the counts of the bathymetric observations along each of the 25 profiles. Each count in turn is squared and divided by the expectation. In this case, it enables to assess the model fit at each of 518 observations for every bathymetric profile for the generalized linear models within the context of the chi–square (Figure 10). It has been computed as a raw residual divided by the square root of the variance function. Technically, association plot method includes execution of the following R code:

library(vcd) # calling necessary package

MDF <– read.csv("Morphology.csv", header=TRUE, sep = ",") # uploading table

MDF <– na.omit(MDF) # deleting non available values in the data frame

row.has.na <– apply(MDF, 1, function(x){any(is.na(x))})

sum(row.has.na) # checking up non available values in the data frame

head(MDF) # visualizing data frame as a table

 # step–2. Merging columns in a table according to their category values (tectonic plates)

MDTt = melt(setDT(MDF), measure = patterns("^plate"), value.name = c("tectonics"))

levels(MDTt$variable) = c("Philippine Plate", "Pacific Plate", "Mariana Plate", "Caroline Plate")

assoc(count, shade=TRUE) # plotting association plot according to the tectonic plates crossing the Mariana Trench.

Analysis of Variance (ANOVA) to Assess Hypothesis Testing

The results have been interpreted on the homogeneity of variance by means of the one–way ANOVA series of tests (Figure 11). Several test methods were executed in this research. The brief description of their advantages and particularities is given below. The Tukey HSD (Tukey Honest Significant Differences) multiple pairwise–comparisons were applied to the ANOVA results. Since the ANOVA test is significant, the Tukey HSD test was computed by R function. TukeyHSD() takes the fitted ANOVA as an argument. This test enabled to perform multiple pairwise–comparison between the means of groups. The library{multcomp} was used to perform a pairwise t–test and to calculate pairwise comparisons between the group levels with the corrections for the multiple testing using R function pairwise.t.test(). The Levene's test was used to analyse the homogeneity of variances at the next step of ANOVA testing by calling function leveneTest() in the {car} package. Comparing to the pairwise t–test, the advantages of the Levene's test is its lesser sensitiveness towards the departures from the normal distribution.

Afterwards, the Welch test was executed in parallel to the oneway.test() in experimental mode. The Welch–test does not require that assumption have been implemented in the function oneway.test() which makes is more suitable comparing to the last one. The Shapiro test was alternatively used to analyse variance of the residuals (Figure 11, upper left). Finally, a non–parametric Kruskal–Wallis rank sum test was applied to finish with a series of ANOVA testing. The results have been interpreted on homogeneity of variance by means of one–way ANOVA tests. Since the p–value (Figure 11) is less than the significance level 0.05, one can conclude that there are significant differences between the groups highlighted with "*" in the model summary, that is four tectonic plates: Philippine, Pacific, Mariana and Caroline. The Tukey multiple pairwise–comparisons test enabled to perform multiple pairwise–comparison between the means of groups and demonstrated 95% family–wise confidence level of the results. The plotted homogeneity of variances of the results is shown in Figure 11.

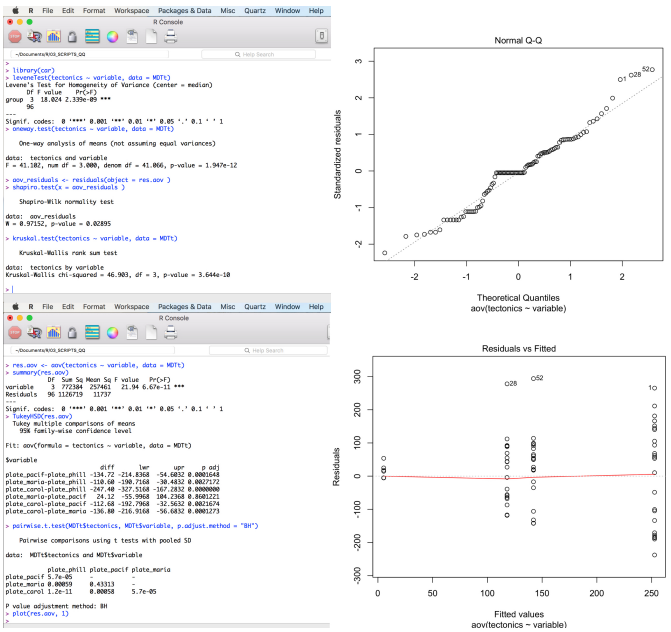

Figure 11. ANOVA hypothesis testing

Results

As can be drawn from the Figure 5, Mariana plate has the highest Kernel density of depth distribution values, followed by the Philippine plate, then Pacific and Caroline, respectively. Kernel density distribution has been shown in a combined plot enabling to compare the overlapping and maximal aptitude of the density curves for both the profiles and depth data distribution by four tectonic plates. The major trend of the trench angles located on the Pacific plate has downward general line trend. The Philippine tectonic plate, on the contrary, has a minimal peak by profiles #14–21, and then moving upwards. The highest value for Caroline plate has profile #23, while the maximal level for Mariana plate has profile #7. The Philippine tectonic plate, on the contrary, has a minimal peak by profiles #14–21, and then moving upwards. The highest value for Caroline plate has profile #23, while the maximal level for Mariana plate has profile #7.

From the composition charts (Figure 8), drawn to compare the slope angles and aspect degree by bathymetric profiles, one can see the unique patters of these categories for the trench. The basic concepts of

the close interrelation of various environmental factors (geological structure, bathymetric patters, tectonic plates location and subduction, spreading, transform fault, depths) affecting Mariana Trench formation is reflected in this paper. The technical tools consist of combination of R programming, GIS spatial analysis and mathematical algorithms for data processing and modelling. A comparison of the properties of the oceanic crust and ophiolite sections, sedimentary thickness and depth distribution across bathymetric profiles enabled to make a better understanding of the ties among geospatial factors influencing Mariana Trench formation. In turn, it facilitate a more reasonable forecast of the possible position of the mineral deposits fossils within Mariana Trench, for instance in the Philippine Sea tectonic plate.

The algorithm based objective analysis of the Mariana Trench bathymetric unevenness enables to better understand its morphology and structure. The special section of this research is focused on the detailed technical evaluation of the R and LaTeX scripts and description of their functionality. The thorough description of the workflow steps is accompanied by the written most important R scripts and codes provided in full, what makes this work repeatable. The discussion of the advantages of the methods enables to have a representative information on the key procedures of the research. As demonstrated in this paper, the combination of the statistical analysis by R programming language, modelling algorithms and GIS geospatial analysis provide the most effective methods for studying ocean floor and hadal trenches, the least reachable research objects on the Earth.

Discussion

The study of the structure of the Mariana Trench has a great scientific and practical interest. First, it relates to the testing theory of plate tectonics. Second, the estimation of the time and place of where earthquakes and tsunami may arise is of great importance for the environmental risk reduction, natural hazard protection and prevention. Moreover, the distribution of the submarine volcanoes is important, as they are one of the principal dynamic forces acting on the Earth's crust. Finally, ocean mining of the deep–seabed mineral resources has enormous economic potential.

The aim of the presented research was to identify bathymetric cross section profiles of the Mariana Trench that show similarity by their complex parameters, so that they could be grouped into patters. Using combination of R programming, LaTeX visualization and GIS, supported by the traditional geologic research, this study enabled to identify variabilities among factors affecting Mariana trench morphology. The accuracy of the performed statistical measurements is impacted by the chosen methodology and the input data: geomorphological maps, geological attribute tables, bathymetric maps, other geospatial thematic layers.

The question of the formation and structure of the ocean trenches has long attracted oceanographers. A variety of research work has been performed applied for various aspects of the hadal trenches: to measure trench depth, to assess the volumes of possible hidden resources in the abyssal depths, to analyse pelagic and biotic communities, to predict earthquakes frequencies. Nowadays, sound statistical methods are elaborated as important additions for traditional GIS methods of geospatial analysis of the deep ocean trenches. Without machine learning algorithms, a geospatial analysis of the big data cannot be considered as accurate and may lead to minor or major shortcomings and errors. Machine learning is therefore indispensable for such remotely located areas as abyssal depths.

The principle of R based geospatial data mining for the ocean research is to perform fusion and integration of multi–source data that allows integration of the heterogeneous information from a variety of sources for the possibility of in–depth analysis. In such a way, a multi–dimensional data processing is possible including following thematic layers: tectonic (continental margin plates), geological (geologic structure), lithological (sedimentation) and oceanological (direction of the deep currents). Automatic reflection of the multi–variant data by the machine learning methods enables to speed up our understanding of the oceans, as well as to increase the accuracy of the research.

Conclusion

The paper presents an application of the R language towards geological studies with a specific case of marine geological features, such as Mariana Trench. The brief sketch on the structure of the main environmental factors of the Mariana Trench has been presented in introduction section, briefly summarizing tectonic plates' movements, geological structure, sediment conditions, bathymetry, lithological properties and other features of the Mariana Trench system. It furthermore reviews the impact of the environmental determinants on the Mariana Trench formation and structure, for instance, the relationship of the transform faults with rift valleys, location of the large igneous polygons. The methodology chapter is focused on the technical approaches of the study of the trench morphology by means of R programming, statistical analysis and GIS. The techniques of the classification are presented, including key R programming scripts. The results chapter highlights the findings received by the application of the technical methods (R programming, statistical algorithms and GIS) with geological analysis of the Mariana Trench seafloor. The graphical and cartographic materials presented in this research support results and findings. Current work demonstrates that the combination of R language, statistical algorithms and Quantum GIS is a highly effective decision for geospatial research aimed at processing multi–dimensional geospatial data sets.

As a recommendation for further research focused on ocean trenches, a traditional methods of the seafloor studies at the GIS level should always include a set of statistical analysis tools such as R, or alternatively, python (e.g. ScyPy, NumPy, matplotlib), Matlab, Octave. Studies of the spatial data series are usually accompanied by the graphics in view of the facetted plots that can facilitate comparison of the data by groups. This is especially useful while collecting multi–dimensional various geophysical data. Since there are many deep interconnections among factors affecting the formation, morphology and development of the trench, mathematical algorithms and objective analyses based approaches are to be used to study marine geo–systems.

Conflict of Interest

The author declares that there is no conflict of interest.

Acknowledgements

The study has been funded by the China Scholarship Council (CSC), State Oceanic Administration (SOA), Marine Scholarship of China [Grant # 2016SOA002, 2016].

References

Butuzova, G. Y. (2003). Hydrothermal–Sedimentary Ore Formation in the World Ocean. *Geos*, Moscow, Russia. 136p.

Dubinin, E. P. & Ushakov, S. A. (2001). Oceanic Rift Genesis. *Geos*, Moscow, Russia. 293p.

Gardner, J. V., Armstrong, A. A., Calder, B. R. & Beaudoin, J. (2014). So, How Deep Is The Mariana Trench? *Marine Geodesy*, ***37***(1): 1–13.

Garfunkel, Z., Anderson, C. A. & Schubert, G. (1986). Mantle Circulation and the Lateral Migration of Subducted Slabs. *Journal of Geophysical Research*, ***91***: 7205–7223.

Gurevich, E. G. (1998). Metalliferous Sediments in the World Ocean. Nauchnyy Mir, Moscow, Russia. 340p.

Horleston, A. C. & Helffrich, G. R. (2012). Constraining Sediment Subduction: A Converted Phase Study of the Aleutians and Marianas. *Earth and Planetary Science Letters*, ***359–360***: 141–151.

Husson, L. (2012). Trench Migration and Upper Plate Strain over a Convecting Mantle. *Physics of the Earth and Planetary Interiors*, ***212–213***: 32–43.

Ishibashi, J., Tsunogai, U., Toki, T., Ebina, N., Gamo, T., Sano, Y., Masuda, H. & Chiba, H. (2015). Chemical Composition of Hydrothermal Fluids in the Central and Southern Mariana Trough Backarc Basin. *Deep–Sea Research Part II: Topical Studies in Oceanography*, ***121***: 126–136.

Lin, J. W. B. (2008). Qtcm 0.1.2: A Python Implementation of the Neelin–Zeng Quasi–Equilibrium Tropical Circulation Model. *Geoscientific Model Development*, ***1***: 315–344.

Marta–Almeida, M., Ruiz–Villarreal, M., Otero, P., Cobas, P., Peliz, A., Nolasco, R., Cirano, M. & Pereira, J. (2011). OOF3: A Python Engine for Automating Regional and Coastal Ocean Forecasts. *Environmental Modelling & Software*, ***26***: 680–682.

Oliphant, T. E. (2007). Python for Scientific Computing. *Computing in Science & Engineering*, ***9***: 10–20.

R Core Team (2018). R: A Language and Environment for Statistical Computing. R Foundation for Statistical Computing, Vienna. https://www.R–project.org

Roberts, J. J., Best, B. D., Dunn, D. C., Treml, E. A. & Halpin, P. N. (2010). Marine Geo–Spatial Ecology Tools: An Integrated Framework for Ecological Geoprocessing with ArcGIS, Python, R, MATLAB, and C++. *Environmental Modelling & Software*, ***25***: 1197–1207.

Uyeda, S. & Kanamori, H. (1979). Back–Arc Opening and the Mode of Subduction. *Journal of Geophysical Research*, ***84***: 2017–2037.

Warner, J. C., Perlin, N. & Skyllingstad, E. D. (2008). Using the Model Coupling Toolkit to Couple Earth System Models. *Environmental Modelling & Software*, ***23***: 1240–1249.

Mar. Sci. Tech. Bull. (2019) 8(1): 10–12

e–ISSN: 2147–9666

info@masteb.com

http://dergipark.gov.tr/masteb

http://www.masteb.com/

DOI: 10.33714/masteb.495110

Marine Science and Technology Bulletin

RESEARCH ARTICLE

Occurrence of *Sudis hyalina* Rafinesque, 1810 (Paralepididae) in Büyükeceli Coast (Mersin Bay, Northeastern Mediterranean)

Deniz Ayas[1] • Nuray Çiftçi[1*] • Mustafa Doğangün[1] • Mısra Bakan[1]

[1] *Mersin University, Faculty of Fisheries, Mersin, Turkey*

ARTICLE INFO

Article History:

Received: 11.12.2018

Received in revised form: 31.01.2019

Accepted: 20.03.2019

Available online: 05.04.2019

Keywords:

Büyükeceli Coast

Sudis hyalina

NE Mediterranean Sea

Mersin Bay

Turkey

ABSTRACT

In November 2018, an individual belonging to the *Sudis hyalina* was caught in a trawling operation in the Büyükeceli Coast (Mersin Bay, NE Mediterranean). Morphological and meristic measurements of the specimen were made and recorded with the catalogue number of MEUFC-18-11-102 in the Museum of the Systematic, Faculty of Fisheries, Mersin University.

Please cite this paper as follows:

Ayas, D., Çiftçi, N., Doğangün, M., Bakan, M. (2019). Occurrence of *Sudis hyalina* Rafinesque, 1810 (Paralepididae) in Büyükeceli Coast (Mersin Bay, Northeastern Mediterranean). *Marine Science and Technology Bulletin*, 8(1): 10–12.

Introduction

Sudis hyalina belongs to the Paralepididae family of Aulopiformes. It is known that *S. hyalina*, a deep-sea fish, has a very wide distribution area between 200-2000 m depth in the mesopelagic and bathypelagic zone (Post, 1990). However, the reproduction of this species usually occurs in tropical and warm shallow waters (Post, 1990). The maximum length of the species reported in the literature is 100 cm for adult individuals, while the total length of young individuals is generally 40 cm (Bauchot, 1987). Their fins do not contain spines.

* Corresponding author

E-mail address: nciftci@mersin.edu.tr (N. Çiftçi)

Total dorsal soft rays: 12-16, total anal soft rays: 21-24. Their body color is silvery pink. The lower jaw of *S. hyalina* is markedly curled up, and its teeth are large and the number is greater than the upper jaw. Gill rakes contain tooth-like structures (Whitehead et al., 1986). The structure of the mouth and teeth reflects the diet of the species. They are carnivore predators (Post, 1990).

The records of the species were done from Levantine Basin by Golani (1996), from Taşucu and Iskenderun Bay by Mater and Kaya (1987) and Kaya and Bilecenoğlu (2000), from the shores of Turkey by Bilecenoğlu et al. (2014), from Mersin Bay by Ergüden and Bayhan (2015), from Gökova Bay, Aegean Sea by Türker et al. (2016), from the Lebanese coast by Tortonese (1970) and from the Syrian coast by Ali et al. (2014) in the Eastern Mediterranean; from the middle and western Mediterranean Sea by Psomadakis et al. (2006), D'Onghia et al. (2011), and Mytilineou et al. (2013).

The aim of this study is to report the new locality record of *S. hyalina* from Büyükeceli coast (Mersin Bay) and to determine the current status of this species in the coast of Turkey.

Material and Methods

One individual of *S. hyalina* Rafinesque, 1810 was caught by a trawl operation at a depth of 365 m on 7 November 2018 in the Büyükeceli Coast (Mersin Bay) (coordinate: 36°05'45.5"N 33°23'20.0"E). This specimen was preserved in 4% formalin and was deposited in the Museum of the Systematic, Faculty of Fisheries, Mersin University, (catalogue number: MEUFC-18-11-102). Morphometric and meristic characters of this specimen are given in Table 1 and sampling point of the species in the Mediterranean Sea is presented in map (Figure 1). Photographs of caught specimen are shown in Figures 2.

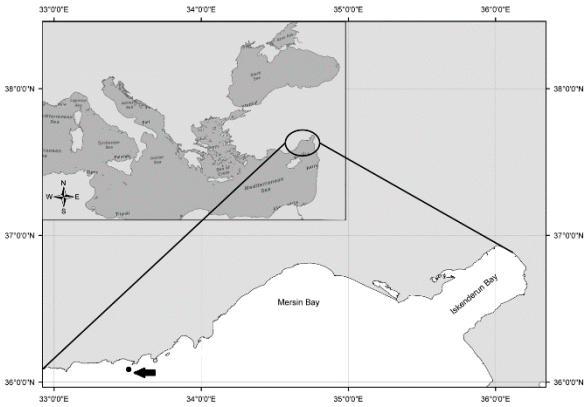

Figure 1. Map showing the capture site off Büyükeceli, Mersin Bay (NE Mediterranean Sea)

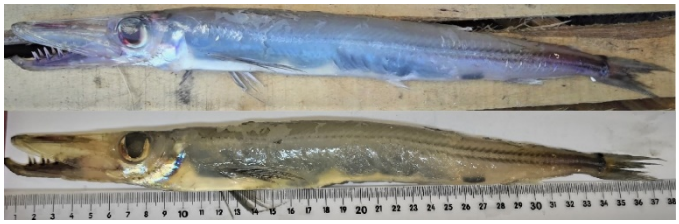

Figure 2. Photographs of *S. hyalina* caught from Büyükeceli Coast

Results

In this study, a young individual (total size of 38.1 cm) of *S. hyalina* was caught from the Büyükeceli coast in November 2018. Some morphometric and meristic measurements of this individual were made and presented in Table 1.

Table 1. Comparison of *S. hyalina* individuals in terms of morphometric and meristic measurements

Measurements (mm)	Present study (n=1)	Ali et al., 2014 (n=2)	
		1st Ind.	2nd Ind.
Morphometric Characters			
Total length	381	358	322
Fork length	344	346	296
Standard length	339	328	282
Head length	105	96	83
Interorbital space	11	11	9
Eye diameter	19	21	16
Preorbital length	69	-	-
Postorbital length	25	-	-
Snout length	46	34	27
Upper jaw length	62	58	52
Lower jaw length	69	64	56
Pectoral fin length	59	62	53
Pectoral fin base	13	12	11
Dorsal fin length	23	26	27
Dorsal fin base	25	23	24
Pelvic fin length	20	24	17
Pelvic fin base	6	4	5
Anal fin length	22	26	22
Anal fin base	43	42	38
Body height	36	36	31
Body depth	22	21	14
Pre-pectoral length	119	119	94
Pre-dorsal length	236	227	193
Pre-pelvic length	117	213	174
Pre-anal length	281	272	234
Pre-adipose fin	287	309	267
Caudal peduncle length	21	-	-
Caudal peduncle depth	12	-	-
Caudal peduncle height	41	-	-
Meristic Characters			
Dorsal fin soft rays	13	13	13
Pelvic fin soft rays	8	8	10
Anal fin soft rays	21	21	20
Pectoral fin soft rays	13	13	15
Caudal fin soft rays	20	16	18
Left and right upper jaw teeth	3+3	2+2	3+3
Left and right lower jaw teeth	8+12	6+8	7+5

Discussion

Morphometric and meristic measurements of the captured individual were compared with the measurements of two individuals of *S. hyalina* that were caught in the coast of Syria by Ali et al. (2014) (Table 1).

The measurements of two individuals caught in Syrian waters were found to be compatible with an individual caught from Mersin Bay. This may be because individuals in both studies had similar size. The

individuals in both studies were also young. The fact that the young individuals belonging to the species are rarely caught in coastal waters during fishing activities may indicate the existence of a population in the Mediterranean, but also the fact that mature individuals only come to the shallow waters for spawning. The reproduction of this species usually occurs in tropical and warm shallow waters (Post, 1990).

S. hyalina has been reported from all over the Mediterranean (Tortonese, 1970; Mater and Kaya, 1987; Golani, 1996; Kaya and Bilecenoğlu, 2000; Psomadakis et al., 2006; D'Onghia et al., 2011; Mytilineou et al., 2013; Ali et al., 2014; Bilecenoğlu et al., 2014; Ergüden and Bayhan, 2015). However, the number of individuals of the species reported in these records is limited. *S. hyalina* is a carnivore predator species and has been continually reported in the Mediterranean over the past 50 years; this may be indicating that the species is not under pressure of predator, fishing, or any other non-indigenous species, and maintains its presence in the Mediterranean. It was thought that the capture of a small number of individuals of *S. hyalina* may be due to the fact that it is a deep sea fish and the adults are present in the bathypelagic zone, except for spawning period.

Conclusion

According to the literature records, *S. hyalina* is a circumglobal species and has been recorded in the Mediterranean Sea for the last 50 years. Therefore, it can be said that the species is permanently found in the Mediterranean fish species list. The Mediterranean Sea is an ecosystem that dynamically changes species diversity due to the Lessepsian migration. Although the earlier records of the species have been reported, additional records are important biodiversity data in terms of the current status of the species in the region, the state of population formation, the examination of the relations between species.

Conflict of Interest

The authors declare that there is no conflict of interest.

Acknowledgements

This study was supported by the Research Fund of Mersin University in Turkey with Project Number: 2017-2-AP2-2353.

References

Ali, M., Saad, A., Reynaud, C. & Capapé, C. (2014). First Records of Barracudina *Sudis hyalina* (Osteichthyes: Paralepididae) off the Syrian Coast (Eastern Mediterranean). *Journal of Ichthyology*, ***54***(10): 786-789.

Bauchot, M. L. (1987). Poissonsosseux. In: Fischer, W., Bauchot, M. L., Schneider, M. (eds.), Fiches FAO d'identification pour les besoins de la pêche. (rev. 1). Méditerranée et merNoire. Zone de pêche 37. Vol. II. Commission des Communautés Européennes and FAO, Rome. pp. 891-1421.

Bilecenoğlu, M., Kaya, M., Cihangir, B. & Çiçek, E. (2014). An Updated Checklist of the Marine Fishes of Turkey. *Turkish Journal of Zoology*, ***38***: 901-929.

D'Onghia, G., Indennidate, A., Giove, A., Savini, A., Capezzuto, F., Sion, L., Vertino, A. & Maiorano, P. (2011). Distribution and Behavior of Deep Sea Benthopelagic Fauna Observed using Towed Cameras in the Santa Maria di Leuca Cold Water Coral Province. *Marine Ecology Progress Series*, ***443***: 95-110.

Ergüden, D. & Bayhan, Y. K. (2015). Three Fish Species Known to be Rare for Turkey, Captured from the Northeastern Mediterranean Coast of Turkey, Mersin Bay, *Sudis hyalina* Rafinesque, *Chlopsis bicolor* Rafinesque, *Squatina aculeata* Cuvier. *International Journal of Scientific and Technological Research*, ***1***(4): 1-8.

Golani, D. (1996). The Marine Ichthyofauna of the Eastern Levant-history, Inventory and Characterization. *Israel Journal of Zoology*, ***42***: 15-55.

Kaya, M. & Bileceoglu, M. (2000). New records of Deep-Sea Fish in Turkish Seas and the Eastern Mediterranean. *Journal of Ichthyology*, ***40***(7): 543-547.

Mater, S. & Kaya, M. (1987). Türkiye'nin Akdeniz Sularinda Yeni Kaydedilen Üç Balik Türü, *Sudis hyalina* Rafinesque, *Pelates quadrilineatus* (Bloch), *Apogon nigripinnis* Cuvier (Teleostei). *Doga-Türk Zooloji Dergisi*, ***11***(1): 45-49.

Mytilineou, C., Anastasopoulou, A., Christides, G., Bekas, P., Smith, C. J., Papadopoulou, K. N., Lefkaditou, E. & Kavadas, S. (2013). New Records of Rare Deep Water Fish Species in the Eastern Ionian Sea (Mediterranean Sea). *Journal of Natural History*, ***47***: 25-28.

Post, A. (1990). Sudidae. In: Quero, J. C., Hureau, J. C., Karrer, C., Post, A., Saldanha, L. (eds.), Check-List of the Fishes of the Eastern Tropical Atlantic (CLOFETA). JNICT, Lisbon; SEI, Paris; and UNESCO, 385p.

Psomadakis, P. N., Scacco, U. & Vacchi, M. (2006). Recent Findings of Some Uncommon Fishes from the Central Tyrrhenian Sea. *Cybium*, ***30***(4): 297-304.

Tortonese, E. (1970). Fauna d'Italia: Osteichthyes (Pesci Ossei). 1st ed. Bologna, Italy: Edizioni Calderini, 565p.

Türker, D., Kara, A., Bal, H. & Tünay, Ö. K. (2017). Occurrence of Rare Deep-Water Fish *Sudis hyalina* Rafinesque, 1810 (Paralepididae) in Gökova Bay, Aegean Sea of Turkey. *Journal of Applied Ichthyology*, ***33***(3): 535-538.

Whitehead, P. J. P., Bauchot, M. L., Hureau, J. C., Nielsen, J. & Tortonese, E. (Eds.) (1986). Fishes of the North-eastern Atlantic and the Mediterranean. Paris, France: UNESCO, ***I-III***: 1473 p.

Mar. Sci. Tech. Bull. (2019) 8(1): 13–22

e–ISSN: 2147–9666

info@masteb.com

http://dergipark.gov.tr/masteb

http://www.masteb.com/

DOI: 10.33714/masteb.480957

RESEARCH ARTICLE

Determination of Usage Potential of Some Mediterranean Rays in Fish Oil Production

Deniz Ayas[1] • Elif Ayşe Erdoğan Eliuz[2*] • Ferit Peri[1] • Mısra Bakan[1]

[1] *Faculty of Fisheries, Mersin University, Mersin, Turkey*

[2] *Department of Food Technology, Vocational School of Technical Sciences, Mersin University, Mersin, Turkey*

ARTICLE INFO

Article History:

Received: 09.11.2018

Received in revised form: 19.03.2019

Accepted: 30.05.2019

Available online: 24.06.2019

Keywords:

Dasyatis pastinaca,
Raja radula,
Raja clavata,
Torpedo marmorata,
Heavy metal,
Fatty acid

ABSTRACT

In this study, it was determined the chemical composition of the four ray species (*Dasyatis pastinaca, Raja radula, Raja clavata* and *Torpedo marmorata*) caught from Mersin Bay in the Northeastern Mediterranean Sea. For this purpose, lipid levels, fatty acid profiles, macro-trace elements, and heavy metal levels in the liver and muscle tissues of the Mediterranean rays were investigated. Lipid levels of liver tissue of *D. pastinaca, R. radula, R. clavata, T. marmorata* were determined to be 80.21%, 53.73%, 45.57% and 45.26%, respectively; while lipid levels for muscle tissue were 1.62%, 1.31%, 1.20% and 1.43%, respectively. In the fatty acid composition of muscle tissues of the rays; ∑SFAs (total saturated fatty acids) levels were reported to be between 30.46% and 35.00%, ∑MUFAs (total saturated fatty acids) levels were 21.49% to 27.77%, ∑PUFAs (total polyunsaturated fatty acids) levels were 28.76% to 35.69%; while for liver tissues; ∑SFAs levels were reported to be between 25.76% and 31.15%, ∑MUFAs levels were 23.43% to 30.66%, ∑PUFAs levels were 21.86% to 30.54%. According to data of this current study, no potential toxic metals (Cr, As, Cd, Pb, Hg) were detected in the fish oils obtained from the tissues. Finally, it was showed that these fish had potential for fish oil production because of their having fat in the liver tissues and there were also no potential heavy metal in the both muscle oil and liver oil, being rather healthy.

Please cite this paper as follows:

Ayas, D., Erdoğan Eliuz, E.A., Peri, F., Bakan, M. (2019). Determination of Usage Potential of Some Mediterranean Rays in Fish Oil Production. *Marine Science and Technology Bulletin*, 8(1): 13–22.

* Corresponding author

E-mail address: eliferdogan81@gmail.com (E.A. Erdoğan Eliuz)

Introduction

Fish is a crucial source of food for human health and easily digestible because of its long muscle fibers. All fish species have fat, high quality protein, essential minerals and vitamins but, above all, significant amounts of omega-3 long-chain poly-unsaturated fatty acids (PUFAs) which are an essentially unique and very essential in human nutrition. PUFAs like eicosapentaenoic (EPA, C20:5n3), arachidonic (C20:4n6) and docosahexaenoic (DHA, C22:6n3) acids which need to be taken from the outside, are not synthesized in the human body (Kaur et al., 2012). The many studies have showed that PUFAs prevent and also potentially alleviate cancer, nervous system, reproductive system and cardiovascular diseases. These fatty acids are well reported mainly in the prevention of those diseases by protecting cell-membrane fluidity, improving functions of vascular endothelial cells, reducing of mild hypertension, decreasing susceptibility to ventricular abnormal heart rhythms, diminishing secretion of proinflammatory cytokines by macrophages, inhibiting blood platelet aggregation (Wiktorowska-Owczarek et al., 2015). Especially, EPA and DHA, critical for human health, both play a crucial role in the prevention of a wide range of disorders such as cancer, coronary heart and cardiovascular diseases (Chan et al., 2005; Navarro-García et al., 2009; Navarro-García et al., 2014). Therefore, there is increasing interest nowadays in fish lipids because of their PUFAs.

Heavy metals, macro and trace elements in commercial seafood are often subject to scientific researches in terms of public health (Fernandes et al., 2007). Especially, minerals such as sodium (Na), magnesium (Mg), potassium (K), calcium (Ca), manganese (Mn), copper (Cu), zinc (Zn), are very helpful for health and complementary nutritional factors of body metabolism (Ayas et al., 2016). While some metal and trace elements have a rather vital role for all living systems, toxic metals such as chromium (Cr), arsenic (As), cadmium (Cd), lead (Pb), mercury (Hg) have a directly harmful effect on human health in above acceptable limits and also are used indicator for the pollution level of the marine ecosystem (Mendil et al., 2010; Authman, 2015; Cresson et al., 2015). Because of the pollutant factors such as transportation ports, heavy marine traffic, industry waste, and other many factories, Northern-Eastern Mediterranean Sea is a risky region for metal pollution (Yılmaz et al., 2017). Therefore, the recent studies showed that fish oils can be a better alternative in terms of health nutrition due to fish tissues may contain relatively high levels of heavy metals (Başusta and Erdem, 2000; Foran et al., 2003; Çoğun et al., 2005).

D. pastinaca is a member of the Chondrichthyes represented by sharks, skates, and rays and most primitive living jawed aquatic vertebrates (Bouchaala et al., 2015). *R. clavata* and *R. radula*, named as thornback, live in sandy and muddy habitats, at depths ranging from shoreward region to 300 m (Saglam and Bascinar, 2008). *R. clavata*, a benthic feeder that prey mainly on crustaceans, is usually found on shelf and upper slope waters at depths between 10-60 m. These species are most common rays encountered by divers (Tufan et al., 2013). *T. marmorata*, known as marbled electric ray, also is a species of Torpedinidae family and commonly found in Mediterranean Sea (Başusta and Erdem, 2000).

Rays were reported to contain a high amount of fat and fatty acid, which is rich in nutrient by Pal et al. (1998), Colakoğlu et al. (2011), and Beckmann et al. (2014). However, there is a little information on the lipid level and fatty acid profiles of thornback rays (*R. radula, R. clavata*) and other rays (*D. pastinaca, T. marmorata*). Therefore, we determined the proximate composition of muscle and liver tissues of the rays caught from Mersin Bay. With the aim of making use of this important resources, the lipid levels of their tissues, fatty acid profiles of their lipids, macro and trace element levels and also the contamination levels with potential toxic heavy metals of lipids from extracted the liver and muscle tissues were investigated.

Material and Methods

Collection and Measurements of Rays

Samplings (*D. pastinaca, R. radula, R. clavata, T. marmorata*) were carried out between Berdan River (36° 43' 31.8" N 34° 54' 27.0" E) and Yeşilovacık Bay (36° 08' 53.6" N 33° 39' 40.7" E) by using a commercial trawler (Figure 1). The sampling was conducted as one season between March 2016 and April 2016 in Mersin Bay, and ray samples were provided in sufficient quantities for each species. Fish were grouped according to species and their sizes (cm) and weights (g) were measured (Table 1).

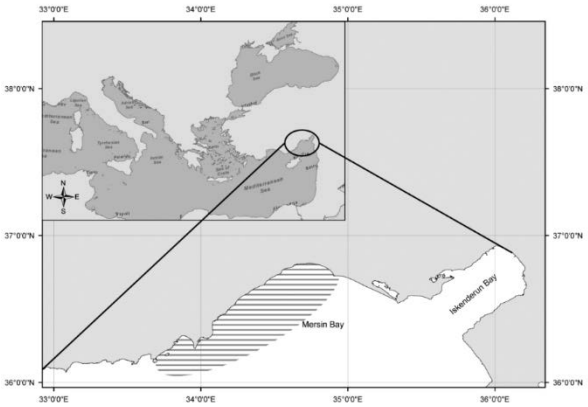

Figure 1. Map of the sampling location (The marked area is the sampling area)

Fat and Fatty Acids Analyses

Lipid content was measured by the method of Bligh and Dyer (1959). In extracted lipids, fatty acid methyl esters were obtained using the Ichihara et al. (1996) method. Fatty acid composition was analyzed using a Gas Chromatography (GC) Clarus 500 device (Perkin–Elmer, USA), one flame ionization detector (FID) and SGE (60 m × 0.32 mm ID BPX70 × 0.25 μm, USA or Australia) column. Injector and detector temperatures were set as 260°C and 230°C respectively. During this time, the furnace temperature was kept at 140°C for 8 minutes. After that, it was increased by 4°C per minute until 220°C, and from 220°C to 230°C by increasing the temperature 1°C per minute. It was kept at 230°C for 15 minutes to complete analysis. Sample scale was 1 μL and carrier gas was controlled at 16 ps. For split flow 40, 0 mL/minute (1:40) level was used. Fatty acids were determined using a comparison to the exit times of the FAME mix that contains 37 standard components.

Table 1. Length and weight of ray samples

Measurements	*D. pastinaca*	*R. radula*	*R. clavata*	*T. marmorata*
N	16	8	7	7
Mean DW (cm)	35.90	33.60	38.14	18.26
Range (cm)	30.0-43.5	32.2-35	37.5-39.0	17.7-19.0
Mean DL (cm)	31.83	32.95	31.51	19.93
Range (cm)	24.5-39.0	31-34.9	30.4-33.0	19.5-20.5
Mean TL (cm)	63.13	54.0	52.5	25.63
Range (cm)	54.0-73.0	51.5-56.5	51-54.5	24.6-27.0
Mean TW (g)	1849.38	895.5	899.86	386.43
Range (g)	955-3205	756-1035	824-1001	368-411
Mean LW (g)	140.16	26.21	27.03	12.30
Range (g)	58.3-265.3	23.01-29.40	21.06-35.0	10.65-14.5
LW/TW*100	7.58	2.93	3.00	3.18

Note: N: Total number of specimens, DW: Disc width, DL: Disc length, TL: Total length TW: Total weight LW: Liver weight.

Atherogenicity Index (AI) and Thrombogenicity Index (TI)

The AI and TI linked to the fatty acid composition were calculated according to Ulbricht and Southgate (1991).

$$AI=\frac{[(a\times 12:0)+(b\times 14:0)+(c\times 16:0)]}{[(d\times(\text{PUFA n-6+n-3}))+(e\times(\text{MUFA}))+(f\times(\text{MUFA-18:1}))]}$$

$$TI=\frac{[g\times(14{:}0+16{:}0+18{:}0)]}{[(h\times(\text{MUFA}))+(i\times(\text{MUFA-18:1}))+(m\times(n-6))+(n\times(n-3))+(n-3/n-6)]}$$

In these formulae; a, c, d, e, f=1; b=4; g=1; h, i, m=0.5; n=3.

Metal Analyses

The samples (0.1 g dry weight) used for metal analysis were dried at 105°C to reach constant weights, and then concentrated nitric acid (4 mL, Merck, Darmstadt, Germany) and percholoric acid (2 mL, Merck, Darmstadt, Germany) were added to the samples, and they were put on a hot plate set to 150°C until all tissues were dissolved (Canli and Atli, 2003).

Inductively coupled plasma mass spectrometer (ICP-MS, Agilent, 7500ce Model, Japan) was used to determine metals. ICP-MS operating conditions were the following: radio frequency (RF) (W), 1500; plasma gas flow rate (L/min),15; auxiliary gas flow rate (L/min), 1; carrier gas flow rate (L/min), 1.1; spray chamber T (°C), 2; sample depth (mm), 8.6; sample introduction flow rate (mL/min), 1; nebuliser pump (rps), 0.1; extract lens (V), 1.5. The levels of macro (Na, Mg, P, K, Ca), trace element (Co, Cu, Zn, Mo, Ni, Se) and potential toxic metal (Cd, Pb) in samples were detected as μg metal g^{-1} dry weight. High Purity Multi Standard (Charleston, SC 29423) was used for determination of the metal analyses. Standard solutions for calibration curves were prepared by dilutions of the macro and trace elements and potential toxic metals. Solutions have prepared for the toxic metals had a content of lead, cadmium, arsenic and chromium in the range of 1-50 ppb (0.001 to 0.050 mg/L), for the macro and trace elements had a content of copper, iron, and zinc in the range of 1-50 ppm (1 to 50 mg/L).

Statistical Analyses

Prior to the analyses, all data were checked for outliers and Levene's homogeneity of variance was also applied for variance homogeneity. Statistical analysis of data was carried out with the IBM SPSS STATISTICS 22 statistical program. ANOVA (Analysis of Variance) was used to evaluate the differences of metals levels of the species.

Results

Some Morphological Measurements of Mediterranean Rays

In this study, the ray samples caught in the Northeastern Mediterranean Sea (Figure 1) were grouped according to species. Four species of rays, *D. pastinaca, R. radula, R. clavata, T. marmorata* have been detected for some physical properties. A total of 38 individuals, total lengths (TL), total weight (TW), liver weight (LW), disc length (DL), disc width (DW) for each ray are presented in Table 1. The means of DW and DL are ranged from 18.26 to 38.14 cm, and from 19.93 to 32.95 cm in the rays, respectively. The means of the TL, TW, and LW for *D. pastinaca* were greater than those of *R. radula, R. clavata, T. marmorata.* The mean TL, TW, and LW were determined to be 63.13 cm, 1849.38 g, 140.16 g for *D. pastinaca*, 54.0 cm, 895.5 g, 26.21 g for *R. radula*, 52.5 cm, 899.86 g, 27.03 g for *R. clavata* and 25.63 cm, 386.43 g, 12.30 g for *T. marmorata*. The highest mean of LW/TW% was found *D. pastinaca* as 7.58%.

The Lipid Levels of the Tissues of Mediterranean Rays

The lipid levels of the liver and muscle tissues of Mediterranean rays are summarized in Table 2. Lipid levels of the liver tissues of *D. pastinaca, R. radula, R. clavata, T. marmorata* were determined to be 80.21%, 53,73%, 45,57% and 45.26%, while lipid levels for muscle tissue were determined to be 1.62%, 1.31%, 1.20% and 1.43%, respectively. The percentages of lipid levels in liver tissues of rays had a significantly higher than in their muscle tissues. Liver tissues of Mediterranean rays are more suitable for fish oil production.

The highest fish oil (80.21%) has been obtained from the liver of *D. pastinaca* (Table 2). The highest mean of LW/TW% was found *D. pastinaca* as 7.58% (Table 1). That's why, the most suitable tissue for fish oil production is the liver tissue of the *D. pastinaca*.

Table 2. The lipid levels of the liver and muscle tissues of Mediterranean rays

Measurements	*D. pastinaca*	*R. radula*	*R. clavata*	*T. marmorata*
Muscle lipid (%)	1.62	1.31	1.20	1.43
Range (%)	1.41-1.76	0.71-1.90	0.95-1.38	1.25-1.57
Liver Lipid (%)	80.21	53.73	45.57	45.26
Range (%)	74.32-85.10	41.90-59.17	40.63-49.28	44.12-46.12

Table 3. The fatty acid profiles of the muscle oil of Mediterranean rays (%)

Fatty Acid	*D. pastinaca* ($\overline{X \pm S_X}$)	*R. radula* ($\overline{X \pm S_X}$)	*R. clavata* ($\overline{X \pm S_X}$)	*T. marmorata* ($\overline{X \pm S_X}$)
C12:0	0.00±0.00^{a}	0.00±0.00^{a}	0.01±0.00^{b}	0.00±0.00^{a}
C14:0	0.26±0.00^{a}	0.47±0.02^{b}	0.59±0.03^{c}	0.76±0.01^{d}
C15:0	0.27±0.00^{a}	0.51±0.00^{b}	0.52±0.02^{b}	0.56±0.01^{c}
C16:0	16.86±0.04^{a}	19.05±0.01^{b}	19.39±0.92^{b}	20.27±0.09^{c}
C17:0	0.84±0.00^{a}	1.69±0.04^{d}	1.40±0.06^{c}	1.10±0.01^{b}
C18:0	9.60±0.00^{c}	8.63±0.02^{b}	8.05±0.41^{a}	10.63±0.06^{d}
C20:0	0.11±0.00^{ab}	0.10±0.00^{a}	0.11±0.01^{b}	0.11±0.00^{b}
C22:0	0.08±0.01^{b}	0.17±0.00^{c}	0.03±0.00^{a}	0.03±0.00^{a}
C24:0	2.44±0.01^{c}	2.23±0.03^{b}	2.21±0.10^{b}	1.54±0.01^{a}
ΣSFA	30.46	32.83	32.31	35.00
C14:1	0.08±0.00^{a}	0.10±0.00^{b}	0.08±0.00^{a}	0.14±0.00^{c}
C15:1	0.12±0.00^{a}	0.18±0.00^{b}	0.13±0.01^{a}	0.28±0.00^{c}
C16:1	2.43±0.01^{c}	1.48±0.03^{a}	1.42±0.07^{a}	2.33±0.01^{b}
C17:1	0.53±0.04^{a}	0.61±0.00^{b}	0.55±0.02^{a}	0.82±0.01^{c}
C18:1n9t	0.49±0.00^{d}	0.33±0.01^{c}	0.24±0.01^{a}	0.28±0.01^{b}
C18:1n9c	7.02±0.00^{a}	7.78±0.02^{b}	9.33±0.47^{c}	10.39±0.06^{d}
C18:1n7	5.01±0.01^{d}	3.72±0.01^{b}	3.34±0.17^{a}	4.79±0.02^{c}
C20:1n9	0.74±0.00^{c}	0.37±0.00^{a}	0.62±0.03^{b}	0.93±0.01^{d}
C22:1n9	11.02±0.06^{c}	7.75±0.03^{b}	5.67±0.28^{a}	5.82±0.02^{a}
C24:1n9	0.33±0.00^{c}	0.15±0.00^{b}	0.11±0.01^{a}	0.10±0.00^{a}
ΣMUFA	27.77	22.47	21.49	25.88
C18:2n6t	0.19±0.00^{b}	0.13±0.00^{a}	0.14±0.01^{a}	0.14±0.00^{a}
C18:2n6c	0.95±0.02^{b}	1.02±0.01^{c}	1.05±0.05^{c}	0.90±0.01^{a}
C18:3n3	0.21±0.10^{b}	0.10±0.00^{a}	0.14±0.01^{a}	0.09±0.00^{a}
C18:3n6	0.40±0.00^{c}	0.25±0.00^{a}	0.31±0.04^{b}	0.52±0.00^{d}
C20:3n3	0.28±0.00^{d}	0.21±0.01^{c}	0.13±0.01^{a}	0.15±0.00^{b}
C20:3n6	0.08±0.00^{a}	0.12±0.00^{b}	0.14±0.01^{b}	0.13±0.01^{b}
C20:4n6	0.39±0.00^{b}	0.48±0.04^{c}	0.47±0.03^{c}	0.34±0.00^{a}
C20:5n3	2.28±0.00^{b}	3.82±0.02^{d}	3.45±0.18^{c}	2.06±0.01^{a}
C22:4n6	5.35±0.00^{d}	2.17±0.02^{c}	1.14±0.07^{b}	1.07±0.01^{a}
C22:6n3	19.84±0.01^{a}	27.05±0.12^{c}	28.39±1.46^{d}	23.03±0.07^{b}
C22:2cis	1.00±0.01^{c}	0.24±0.00^{a}	0.33±0.02^{b}	0.33±0.00^{b}
ΣPUFA	30.97	35.59	35.69	28.76
SFA/PUFA	0.98	0.92	0.91	1.22
Σn7	5.01	3.72	3.34	4.79
Σn6	7.36	4.17	3.25	3.10
Σn3	22.61	31.18	32.11	25.33
Σn9	19.60	16.38	15.97	17.52
n6/n3	0.33	0.13	0.10	0.12
n3/ n6	3.07	7.48	9.88	8.17
DHA/EPA	8.70	7.08	8.22	11.18
AI	0.24	0.31	0.33	0.36
TI	0.28	0.23	0.22	0.30
Unidentified	10.80	9.09	10.51	10.36

Note: ($\overline{X \pm S_X}$) means Average ± Standard deviation

Fatty Acid Profiles of Mediterranean Rays

Detailed fatty acid profiles of muscle and liver oils of Mediterranean rays are listed in Table 3 and Table 4, respectively. The fatty acid profiles of muscle oil and liver oil obtained from *D. pastinaca, R. radula, R. clavata, T. marmorata* were compared.

The percentages of ΣSFAs in muscle tissues of the rays were reported to be between 30.46% and 35.00%, ΣMUFAs levels were 21.49% to 27.77%, ΣPUFAs levels were 28.76% to 35.69%; while for liver oils; ΣSFAs levels were reported to be between 25.76% and 31.15%, ΣMUFAs levels were 23.43% to 30.66%, ΣPUFAs level were 21.86% to 30.54% The lipidic fractions contained a high amount of PUFAs (up to 50% of the total), mainly composed of C22:6*n*3, C20:5*n*3, C22:4n6, C20:4*n*6, C20:3*n*3, C18:3*n*6, C18:3*n*3, C18:2*n*6, C18:2*n*6, in total fatty acid methyl esters (ΣFAMEs).

Table 4. The fatty acid profiles of the liver oil of Mediterranean rays (%)

Fatty Acid	*D. pastinaca* ($\overline{X} \pm S_X$)	*R. radula* ($\overline{X} \pm S_X$)	*R. clavata* ($\overline{X} \pm S_X$)	*T. marmorata* ($\overline{X} \pm S_X$)
C12:0	0.05±0.00^{b}	0.08±0.01^{c}	0.04±0.01^{b}	0.02±0.00^{a}
C14:0	1.56±0.01^{ab}	1.71±0.06^{b}	2.03±0.03^{c}	1.40±0.39^{a}
C15:0	0.98±0.01^{a}	1.15±0.04^{b}	0.87±0.01^{a}	0.92±0.23^{a}
C16:0	14.58±0.04^{a}	14.68±0.57^{a}	16.07±0.24^{a}	14.81±3.80^{a}
C17:0	1.20±0.00^{a}	1.88±0.11^{b}	1.32±0.02^{a}	1.26±0.32^{a}
C18:0	5.69±0.01^{a}	9.73±0.44^{c}	6.16±0.10^{ab}	6.52±1.62^{b}
C20:0	0.29±0.00^{c}	0.48±0.03^{d}	0.27±0.01^{bc}	0.22±0.06^{a}
C22:0	0.08±0.00^{b}	0.03±0.00^{a}	0.15±0.00^{c}	0.05±0.01^{a}
C24:0	1.33±0.00^{a}	1.41±0,06^{a}	1,53±0.02^{a}	1.91±0.49^{b}
ΣSFA	25.76	31.15	28.44	27.11
C14:1	0.28±0.01^{c}	0.22±0.01^{b}	0.26±0.01^{c}	0.15±0.04^{a}
C15:1	0.46±0.01^{c}	0.28±0.01^{b}	0.25±0.01^{b}	0.12±0.03^{a}
C16:1	6,03±0.02^{c}	3.75±0.15^{a}	4.64±0.07^{b}	3.46±0.93^{a}
C17:1	1.00±0.00^{c}	0.93±0.04^{ab}	0.80±0.01^{a}	0.97±0.24^{bc}
C18:1n9t	0.71±0.00^{d}	0.44±0.02^{c}	0.34±0.00^{b}	0.23±0.06^{a}
C18:1n9c	11.27±0.02^{a}	11.27±0.47^{a}	14.10±0.23^{b}	11.01±2.83^{a}
C18:1n7	4.49±0.01^{b}	3.95±0.17^{ab}	3.85±0.06^{ab}	3.83±0.99^{a}
C20:1n9	0.90±0.00^{b}	0.65±0.03^{a}	1.22±0.02^{c}	0.80±0.22^{ab}
C22:1n9	5.46±0.02^{c}	6.25±0.28^{d}	4.03±0.06^{b}	2.74±0.70^{a}
C24:1n9	0.06±0.00^{a}	0.11±0.01^{b}	0.05±0.00^{a}	0.12±0.03^{b}
ΣMUFA	30.66	27.85	29.54	23.43
C18:2n6t	0.09±0.00^{a}	0.19±0.01^{bc}	0.21±0.00^{c}	0.15±0.04^{b}
C18:2n6c	1.22±0.01^{a}	1.55±0.07^{b}	1.49±0.03^{b}	1.09±0.28^{a}
C18:3n3	0.26±0.01^{b}	0.30±0.01^{c}	0.27±0.01^{bc}	0.20±0.06^{a}
C18:3n6	0.38±0.00^{ab}	0.47±0.02^{b}	0.35±0.02^{a}	0.45±0.13^{b}
C20:3n3	0.24±0.00^{b}	0.21±0.01^{ab}	0.18±0.00^{a}	0.21±0.06^{ab}
C20:3n6	0.31±0.01^{b}	0.25±0.01^{a}	0.39±0.01^{c}	0.31±0.08^{b}
C20:4n6	0.89±0.01^{c}	0.83±0.03^{c}	0.71±0.01^{b}	0.39±0.10^{a}
C20:5n3	5.30±0.01^{b}	9.14±0.40^{c}	5.72±0.10^{b}	2.64±0.68^{a}
C22:4n6	3.32±0.01^{c}	1.09±0.05^{b}	0.69±0.01^{a}	1.19±0.30^{b}
C22:6n3	8.79±0.02^{a}	13.69±0.62^{b}	20.21±0.33^{c}	17.71±4.57^{b}
C22:2cis	1.06±0.01^{b}	0.28±0.01^{a}	0.32±0.00^{a}	0.27±0.07^{a}
ΣPUFA	21.86	28.00	30.54	24.61
SFA/PUFA	1.18	1.11	0.93	1.10
Σn7	4.49	3.95	3.85	3.83
Σn6	6.21	4.38	3.84	3.58
Σn3	14.59	23.34	26.38	20.76
Σn9	18.40	18.72	19.74	14.90
n6/n3	0.43	0.19	0.15	0.17
n3/ n6	2.35	5.33	6.87	5.80
DHA/EPA	1.66	1.50	3.53	6.71
AI	0.32	0.32	0.34	0.33
TI	0.30	0.26	0.23	0.26
Unidentified	21.76	13.00	11.48	24.85

Note: ($\overline{X} \pm S_X$) means Average ± Standard deviation

Among the SFAs, those occurring at the highest proportions in muscle oil were palmitic acid (C16:0), 20.27% for *T. marmorata*, 19.39% for *R. clavata*, 19.05% for *R. radula*, 16.86% for *D. pastinaca* followed by stearic acid (C18:0) 10.63% for *T. marmorata*, 9.60% for *D. pastinaca,* 8.63% for *R. radula*, 8.05% for *R. clavata.* The most abundant MUFAs found in muscle oils of all samples were C22:1n9, 11.02% for *D. pastinaca,* 7.75% for *R. radula,* 5.82% for *T. marmorata*, 5.67% for *R. clavata*; C18:1*n*9c, 10.39% for *T. marmorata*, 9.33% for *R. clavata*, 7.78% for *R. radula*, 7.02% for *D. pastinaca* and C18:1*n*7, 5.01% for *D. pastinaca,* 4.79% for *T. marmorata,* 3.72% for *R. radula,* 3.34% for *R. clavata.* The percentages of PUFAs found in muscle of the studied ray species were important. EPA (C20:5n3), and DHA (C22:6*n*3), the major n-3 of PUFAs of the muscle tissues, were determined to be 2.06% and 23.03% for *T. marmorata*, 3.45% and 28.39% for *R. clavata*, 3.82% and 27.05% for *R. radula*, 2.28% and 19.84% for *D. pastinaca,* respectively.

AI values were between 0.24 and 0.36 in the muscle oils, and between 0.32 and 0.34 in the liver oils. The highest AI value was in the muscle of *T. marmorata* (0.44) and in the liver oil of *R. clavata* (0.34).

Table 5. Macro-trace elements and heavy metal levels of the tissues of the Mediterranean rays (μg g^{-1})

Elements	*D. pastinaca* ($\overline{X} \pm S_X$)	*R. radula* ($\overline{X} \pm S_X$)	*R. clavata* ($\overline{X} \pm S_X$)	*T. marmorata* ($\overline{X} \pm S_X$)	*Tissue*
Na	3950.64±373.50^{a,y}	3365.60±842.70^{a,x}	10627.43±449.97^{c,y}	7720.04±100.03^{b,x}	*Muscle*
	1338.30±330.94^{a,x}	2051.93±268.19^{ab,x}	3028.69±50.01^{b,x}	7214.95±50.23^{c,x}	*Liver*
Mg	759.20±96.59^{a,y}	1350.39±250.94^{b,y}	822.85±22.11^{a,y}	800.76±10.07^{a,y}	*Muscle*
	0.35±0.01^{a,x}	0.32±0.01^{a,x}	0.29±0.01^{a,x}	0.32±0.02^{a,x}	*Liver*
P	7570.53±426.70^{a,y}	6500.16±734.76^{a,y}	10356.34±301.45^{b,y}	5828.01±99.87^{a,y}	*Muscle*
	2823.01±299.85^{a,x}	3134.10±99.14^{a,x}	3082.65±53.24^{a,x}	3277.31±147.09^{a,x}	*Liver*
K	14095.17±1397.87^{a,y}	9559.93±373.51^{a,y}	28546.95±500.27^{b,y}	11107.98±478.83^{a,y}	*Muscle*
	4231.31±507.93^{a,x}	4789.51±122.84^{a,x}	6182.47±97.08^{a,x}	7201.11±476.43^{a,x}	*Liver*
Ca	608.65±25.50^{a,x}	474.16±161.71^{a,x}	492.63±9.78^{a,x}	829.09±23.89^{b,x}	*Muscle*
	757.81±53.79^{a,x}	614.18±198.02^{a,x}	543.52±15.44^{a,x}	1378.97±98.99^{b,y}	*Liver*
Cr	2.96±0.43^{b,x}	2.96±0.97^{b,x}	4.76±0.15^{b,y}	0.35±0.02^{a,x}	*Muscle*
	1.94±0.75^{a,x}	0.50±0.38^{a,x}	0.91±0.05^{a,x}	1.52±0.05^{a,y}	*Liver*
Mn	0.62±0.06^{a,x}	0.83±0.05^{a,x}	0.83±0.03^{a,x}	0.85±0.05^{a,x}	*Muscle*
	1.82±0.25^{a,y}	2.25±0.12^{a,y}	2.98±0.14^{b,y}	1.87±0.10^{a,y}	*Liver*
Cu	2.42±0.31^{b,x}	0.74±0.10^{ab,x}	0.35±0.03^{a,x}	0.60±0.05^{ab,x}	*Muscle*
	3.24±0.31^{a,x}	13.08±2.24^{d,y}	10.37±0.35^{c,y}	6.25±0.09^{b,y}	*Liver*
Zn	12.61±0.53^{bc,x}	14.23±0.50^{c,x}	9.24±0.49^{a,x}	11.83±0.95^{ab,x}	*Muscle*
	13.83±1.75^{a,x}	24.60±4.99^{b,x}	22.30±1.57^{b,y}	14.26±0.26^{a,x}	*Liver*
As	123.07±25.74^{a,y}	138.98±34.00^{a,x}	800.56±19.78^{b,y}	64.52±2.56^{a,x}	*Muscle*
	41.06±6.44^{a,x}	69.74±18.60^{ab,x}	119.14±9.77^{b,x}	43.73±0.99^{a,x}	*Liver*
Se	9.94±1.23^{b,x}	2.93±0.56^{a,x}	5.26±0.20^{b,x}	2.90±0.26^{a,x}	*Muscle*
	8.00±1.08^{c,x}	2.74±0.41^{a,x}	5.38±0.29^{bc,x}	4.57±0.33^{ab,x}	*Liver*

Note: Values in same rows and columns in each metals with different letters are significantly different ($p<0.05$)

($\overline{X} \pm S_X$) means Average ± Standard deviation

Table 6. The levels of the potential toxic metal in the muscle and liver oils (μg g^{-1})

Elements	*D. pastinaca* ($\overline{X} \pm S_X$)	*R. radula* ($\overline{X} \pm S_X$)	*R. clavata* ($\overline{X} \pm S_X$)	*T. marmorata* ($\overline{X} \pm S_X$)	*Oil*
Cr	ND	ND	ND	ND	*Muscle*
	ND	ND	ND	ND	*Liver*
As	ND	ND	ND	ND	*Muscle*
	ND	ND	ND	ND	*Liver*
Cd	ND	ND	ND	ND	*Muscle*
	ND	ND	ND	ND	*Liver*
Pb	ND	ND	ND	ND	*Muscle*
	ND	ND	ND	ND	*Liver*
Hg	ND	ND	ND	ND	*Muscle*
	ND	ND	ND	ND	*Liver*

Note: ($\overline{X} \pm S_X$) means Average ± Standard deviation; ND means not detected

The Macro Elements, Trace Elements and Toxic Heavy Metal Contents of the Ray Samples

Macro (Na, Mg, P, K and Ca), trace element (Cu, Mn and Se) contents of livers and muscles from the studied species (*D. pastinaca, R. radula, R. clavata, T. marmorata*) are illustrated in Table 5. The relationship between the amounts of macro elements in muscle tissue of *D. pastinaca* and *R. radula* were determined to be K>P>Na>Mg>Ca and K> Na> P >Mg>Ca for *R. clavata, T. marmorata*. In addition, in liver tissues, the relationship between the macro element levels of *D. pastinaca*, *R. radula* and *R. clavata* were measured to be K>P>Na>Ca>Mg and Na >K> P>Ca>Mg for *T. marmorata*. K was the most abundant macronutrient for all ray species and the highest values (14095.17±1397.87, 9559.93±373.51, 28546.95±500.27, 11107.98±478.83 µg/g) were observed for muscle tissues. The other macro elements were also detected at much higher levels in muscle from the fishes compared to that of liver.

Discussion

In the present study, the TL (total length) of *D. pastinaca* ranged from 54.0 to 73.0 cm, and W (weight) was between 955 and 3205 g. Its measurements were reported by Yeldan et al. (2009), TL and W ranged 14.6 to 100.9 cm and 22.5 to 6800 g, respectively. Ismen (2003) reported that the total length of *D. pastinaca* females ranged from 20.5 to 88 cm, and of its males from 20 to 73 cm caught in Iskenderun Bay. Maximum total length observed in our study for *R. clavata* (54.5 cm) were slightly smaller than found in a study carried out (73.2 cm) in the Southeastern Black Sea (Demirhan et al., 2005). Kadri et al. (2013) reported that the TL of *R. radula* collected from the Gulf of Gabes (southern Tunisia, central Mediterranean Sea) ranged from 13.4 to 65 cm, similar to our report (51.5 to 56.5 cm). The average total length and weight of *T. marmorata* collected from North-Eastern Mediterranean were detected to be between 12.26 to 40 cm, 40.40 to 1062.00 g, respectively by Duman and Basusta (2013). According to the study of Filiz and Bilge (2004), *T. marmorata* ranged between 9.2 to 34.3 cm in TL and 14.88 to 862.11 g in W; between 20.5 to 99.0 cm in TL and 28.86 to 2614.28 g in W for *R. clavata*; and 37.3 to 74.2 cm in TL and 333.23 to 2955.0 g in W for *D. pastinaca* in the North Aegean Sea. These measurements were close to our results (mean TL=25.63, mean TW=386.43).

Various factors such as seasons, years, climate, temperature, nutrient, reproductive cycle period, salinity, geographical location, sex and maturity may be responsible for the differences in parameters of oil yield, length and weight of the fish (Olusoji et al., 2010). In our study, we reported that the lipid levels were to be 80.21%, 53,73%, 45,57%, 45.26% in liver and 1.62%, 1.31%, 1.20%, 1.43% in muscle tissue for *D. pastinaca, R. radula, R. clavata, T. marmorata*, respectively. Compared to the lipid content of muscle, the livers of all rays contains significant lipid content. Colakoglu et al. (2011) reported that total lipid content of *R. clavata* was 3.39%. The liver oil level for *D. brevis* was reported 25–50% by Navarro-Garcia et al. (2004). The lipid levels of liver of *D. bleekeri* were reported as 63.4% from the coastal region of West Bengal, India (Pal et al., 1998). Liver oil level for *D. americana* from the Gulf of Mexico (Navarro-Garcia et al., 2009) and *D. dipterura* from Sinaloa of Mexico (Navarro-Garcia et al., 2014) were 38.2% and 46.41%, respectively. In the present study, liver oil of *D. pastinaca* was 80.21%. This level is higher than the results obtained in other studies. This may be due to differences of the ray species and regional differences.

The most abundant SFAs found in liver oil of all rays were palmitic acid, 16.07% for *R. clavata,* 14.81% for *T. marmorata,* 14.68% for *R. radula,* 14.58% for *D. pastinaca and* stearic acid (C18:0), 9.73% for *R. radula,* 6.52% for *T. marmorata,* 6.16% for *R. clavata,* 5.69% for *D. pastinaca.* Among the MUFAs, those occurring at the highest proportions in liver oil were oleic acid, 14.10% for *R. clavata,* 11.27% for *R. radula,* 11.27% for *D. pastinaca,* 11.01% for *T. marmorata* followed by C18:1n7 and C22:1n9, 4.49% and 5.46% for *D. pastinaca,* 3.95% and 6.25% for *R. radula,* 3.85% and 4.03% *R. clavata,* 3.83% and 2.74% for *T. marmorata*. EPA (C20:5n3) and DHA (C22:6n3), the major n-3 of PUFAs, in the liver oils of fishes were determined to be 5.30% and 8.79% for *D. pastinaca,* 9.14% and 13.69% for *R. radula,* 5.72% and 20.21% for *R. clavata,* 2.64% and 17.71% for *T. marmorata*, respectively.

The primary SFA was palmitic acid (C16:0; 26.45%) in muscle oil of *R. clavata*, palmitic acid was followed by stearic acid (C18:0; 10.62%) in *R. clavata* (Turan, 2007). Fernandez-Reiriz Pastoriza and Sampedro, (1992) previously had reported that the main SFAs in *R. clavata* was stearic acid followed by palmitic acid. The palmitic acid and stearic acid were found to be the major SFAs in different fish species (Jabeen and Chaudhry, 2011). Their study demonstrated *Oreochromis mossambicus*, *Cyprinus carpio* and *Labeo rohita* from the Indus River contained reasonable amounts of essential PUFAs such as eicosapentaenoic, docosahexaenoic, and arachidonic acids (Jabeen and Chaudhry, 2011).

The percentages of total SFA and PUFA levels in muscle oil of rays were observed to be higher than those in liver oil. Differences were also determined in the fatty acid profiles. The percentages of ΣMUFAs in liver oil of *D. pastinaca, R. radula, R. clavata* were higher than those in the muscle oil, whereas the ΣMUFAs level in liver oil of *T. marmorata* was lower than in the muscle oil. Moreover, the fatty acid composition of these fishes showed a relatively high ratio of SFA/PUFA in muscle and liver oils; for *D. pastinaca*: 0.98 and 1.18, *R. radula*: 0.92 and 1.11, *R. clavata:* 0.91 and 0.93, *T. marmorata:* 1.22 and 1.10, respectively. The fatty acid profiles of both muscle and liver oils showed to be predominant C16:0 (14.58–20.27%), followed by C22:6*n*−3, (8.79–28.39%).

With regard to n-3 PUFAs, we reported that C20:5*n*3 and C22:6*n*3, the major n-3 of PUFAs, in the liver oils of rays were determined to be 5.30% and 8.79% for *D. pastinaca,* 9.14% and 13.69% for *R. radula,* 5.72% and 20.21% for *R. clavata,* 2.64% and 17.71% for *T. marmorata*, respectively. In another studies, the concentration of the EPA and DHA were found 5.3 and 4.8 g/100 g liver oil in *Dasyatis brevis*, 5.9 and 10.0 g/100 g liver oil in *Gymnura marmorata*. G. (Navarro-Garcia et al., 2004). Similar levels with our study of EPA had been reported in liver oil of *R. clavata.* (Ozyilmaz, 2016). High proportions of DHA

were detected in muscle and liver of *Dasyatis marmorata* (11.1% and 16.1%, respectively) caught from the East Tropical Atlantic Ocean (Ould El Kebir et al., 2003).

In our study, the major *n*-3 of PUFAs, were determined to be 2.06% and 23.03% for *T. marmorata*, 3.45% and 28.39% for *R. clavata*, 3.82% and 27.05% for *R. radula*, 2.28% and 19.84% for *D. pastinaca,* respectively. In the other hand, the concentration of the DHA (C22:6n3) in all the rays was seven times higher than the EPA (C20:5n3). Colakoglu et al. (2011) detected that *n*-3 and *n*-6 PUFAs of *R. clavata* were higher compared to those of spiny dogfish. Beckmann et al. (2014) reported that fish oil or poultry oil-fed *Heterodontus portusjacksoni* sharks showed significant differences in the muscle and liver FA profiles in different times (6, 12, 18 weeks). In control groups, the SFA, PUFA and MUFA were detected 32.5%, 36.0%, 31.6% in liver oils and 36.3%, 35.7%, 28.0% in muscle oils, respectively. When compared to other studies, the most abundant fatty acids in liver and muscle oils of *Salmo trutta macrostigma* caught from Tohma River were found to be palmitic acid, stearic acid, oleic acid, EPA and DHA (Akpinar et al., 2009). Navarro-Garcia et al. (2010) reported that liver oils from both ray species (*Rhinoptera bonasus* and *Aetobatus narinari*) had similar EPA + DHA contents (13.2 and 8.0, respectively).

It was suggested that the *n*3/*n*6 (1:1) ratio is a sufficient index in comparing relative nutritional value of fatty acids of different fish species (Turan, 2007). As our study, the *n*3/*n*6 ratio of the rays was found between 3.07 and 9.88 in muscle oils, while between 2.35 and 6.87 in liver oils.

The lowest TI value determined in the muscle oil of *R. radula* and both muscle and liver oils of *R. clavata* were 0.23. The highest TI value was in the liver oil of *D. pastinaca* (0.30). From these results, we detected that both muscle and liver oils had greatly atherogenic and thrombogenic indices. In another study, Jankowska et al. (2010) reported the AI values were between to be 0.38 and 0.70, while TI values were between to be 0.24 and 0.34 in the muscle, liver, and mesenteric fat of *Perca fluviatilis.*

When comparing with the present study, Türkmen et al. (2014) measured similar Pb, Mn, Cu, and Cd in livers of *T. marmorata, D. pastinaca,* and *R. radula*. Heavy toxicity metals such as As, Cd, Hg and Pb are among the most serious elements of marine pollution worldwide, given their persistency in the environment and bioaccumulation. These elements are released to the nature through natural and/or artificial processes, including agriculture, mining, industrial and urban discharges (Ansari et al., 2004). When it reaches human body, several toxicological such as immunotoxicity, teratogenicity, endocrine toxicity and carcinogenetic promotion occurred. (Ahlborg et al., 1994). When metal varies that accumulated by aquatic organisms are excessively intake to human body, they cause diseases in metabolism due to their toxicity (Foran et al., 2003). In our study, we reported that there is no information about Cd, Pb, Cr, As, Hg metals in any oil samples extracted from liver and muscle. Similarly, Rubio-Rodríguez et al. (2012) reported that heavy metals (Cd, Hg, Pb, As) in fish oil extracted from livers of *Merluccius paradoxus*, *Hoplostethus atlanticus*, and *Salmo salar* were to be negligible. In the study of Foran et al. (2003), they have shown that the levels of mercury in the 5 commercial brands of fish oil ranged from non-detectable (6 mg/L) to negligible (10–12 mg/L). Also, they have expressed that consumption of fish oil were safer alternative to fish preparations (Foran et al., 2003).

In the studied on tissues, according the study of Canli and Atli (2003), the concentrations of Cu (202.8), Cd (4.50), Cr (17.1) and Pb (41.2) were detected in liver tissues of *Mugil cephalus, Trigla cuculus*, *Sardina pilchardus* and *Atherina hepsetus*, respectively. Bat and Arici (2016) presented that toxic element limit values of Atlantic bonito (*Sarda sarda*) caught in the Black Sea were edible levels. Gümgüm et al. (1994) were not detected Co, Mo, Pb and V accumulation in *Cyprinion macrostomus* and *Garra rufa* from Tigris River by Ergani Copper Plant and the geochemical structure of this region. Studies have reported that Pb and Cd accumulation levels of marine fish were in the following orders: Gonads > Skin > Gill > Liver > Muscle according to Masoud et al. (2007) and Spleen > Kidney > Liver > Gill > Muscle according to Çoğun et al. (2005). Anyway, mean value of As levels in *Sardinia lascaris* were Liver > Muscle > Skin, and in *Trachurus lucerna*, Muscle > Liver > Skin (Juresa and Blanusa, 2003).

The liver and muscle tissues of fish are generally contaminated with toxic metals. However, in this study we have reported that heavy metals in the oils extracted from liver and muscle tissues from *D. pastinaca, R. radula, R. clavata, T. marmorata* were to be below the limit of detection and not contain a significant amount of them. Therefore, the oils extracted from these species are suitable for human consumption in terms of metal contamination and risk of toxicity.

Conclusion

This study compared the fat and fatty acid composition, macro and trace element levels of the muscle and liver tissues of *R. radula*, *R. clavata*, *D. pastinaca*, *T. marmorata* and also the contamination levels with potential toxic heavy metals of oils of their tissues. Lipid contents of all the species were reported as sufficient for human health. The results show that rays are potential resources of polyunsaturated fatty acids (PUFAs) and should be used in the diet of local populations. They contained essential macro and trace elements, fatty acids, which are very crucial for health. Finally, these fish have potential for fish oil production because of their having no toxic heavy metal in the oils extracted their liver and muscle tissues. Especially, It was determined that the most suitable tissue for fish oil production is liver tissue of *D. pascinata* in terms of its oil level, size or weight and also having none heavy metal risk of its oils.

Acknowledgements

This study was supported by the Research Fund of Mersin University in Turkey with Project Number: 2017-1-TP2-2173.

Conflict of Interest

The authors declare that there is no conflict of interest.

References

Ahlborg, U. G., Becking, G. C., Birnbaum, L. S., Brouwer, A., Derks, H. J. G. M., Feeley, M., Golor, G., Hanberg, A., Larsen, J. C., Liem, A. K. D., Safe, S. H., Schlatter, C., Waern, F. J. M. & Yrjanheikki, E. (1994). Toxic equivalency factors for dioxin-like PCBs. Report on WHO-ECEH and IPCS Consultation, December 1993. *Chemosphere,* ***28***(6): 1049-1067.

Akpinar, M. A., Görgün, S. & Akpinar, A. E. (2009). A comparative analysis of the fatty acid profiles in the liver and muscles of male and female *Salmo trutta macrostigma*. *Food Chemistry,* **112**(1): 6-8.

Ansari, T. M., Marr, I. L. & Tariq, N. (2004). Heavy metals in marine pollution perspective: A mini review. *Journal of Applied Sciences*, ***4***(1): 1-20.

Authman, M. M. (2015). Use of fish as bio-indicator of the effects of heavy metals pollution. *Journal of Aquaculture Research and Development*, ***6***(4):1-13.

Ayas, D. Köşker, A. R., Durmuş, M. & Bakan, M. (2016). Determination of seasonal changes on some heavy metal (Cd, Pb, Cr) levels of shrimp and prawn species from north-eastern Mediterranean Sea, Gulf of Mersin, Turkey. *Journal of Aquaculture Engineering and Fisheries Research,* ***2***(2): 42-49.

Başusta, N. & Erdem, U. (2000). A study on the pelagic and demersal fishes of Iskenderun Bay. *Turkish Journal of Zoology,* ***24***(1): 1–20.

Bat, L. & Arici, E. (2016). Health risk assessment of heavy metals in *Sarda sarda* Bloch, 1793 for people through consumption from the Turkish Black Sea coasts. *International Journal of Zoology Research,* ***1***(1): 1–7.

Beckmann, C. L., Mitchell, J. G., Stone, D. A. J. & Huveneers, C. (2014). Inter-tissue differences in fatty acid incorporation as a result of dietary oil manipulation in Port Jackson sharks (*Heterodontus portusjacksoni*). *Lipids,* ***49***(6): 577–590.

Bligh, E. G. & Dyer, W. J. (1959). A rapid method of total lipid extraction and purification. *Canadian Journal of Biochemistry and Physiology,* ***37***(8): 911–917.

Bouchaâla, E., BouAli, M., Ali, Y., Ben Miled, N., Gargouri, Y. & Fendri, A. (2015). Biochemical characterization and molecular modeling of pancreatic lipase from a cartilaginous fish, the common stingray (*Dasyatis pastinaca*). *Applied Biochemistry and Biotechnology,* ***176***(1): 151–169.

Canli, M. & Atli, G. (2003). The relationships between heavy metal (Cd, Cr, Cu, Fe, Pb, Zn) levels and the size of six Mediterranean fish species. *Environmental Pollution,* ***121***(1): 129–136.

Chan, J. M., Gann, P. H., Giovannucci, E. L. (2005). Role of diet in prostate cancer development and progression. *Journal of Clinical Oncology,* ***23***(32): 8152–8160.

Colakoglu, F. A., Ormanci, H. B. & Cakir, F. (2011). Effect of marination and smoking on lipid and fatty acid composition of thornback ray (*Raja clavata*) and spiny dogfish (*Squalis acanthias*). *European Food Research and Technology,* ***232***(6): 1069–1075.

Çoğun, H., Yüzereroğlu, T. A., Kargin, F. & Firat, Ö. (2005). Seasonal variation and tissue distribution of heavy metals in shrimp and fish species from the Yumurtalik Coast of Iskenderun Gulf, Mediterranean. *Bulletin of Environmental Contamination and Toxicology,* ***75***(4): 707–715.

Cresson, P., Bouchoucha, M., Miralles F., Elleboode, R., Mahe, K., Marusczak, N., Thebault, H. & Cossa, D. (2015). Are red mullet efficient as bio-indicators of mercury contamination? A case study from the French Mediterranean. *Marine Pollution Bulletin*, ***91***(1): 191–199.

Demirhan, S. A., Engin, S., Seyhan, K. & Akamca, E. (2005). Some biological aspects of thornback ray (*Raja clavata* L., 1758) in the southeastern Black Sea. *Turkish Journal of Fisheries and Aquatic Sciences*, ***5***(2): 75-83.

Duman, O. & Basusta, N. (2013). Age and growth characteristics of marbled electric ray *Torpedo marmorata* (Risso, 1810) inhabiting Iskenderun Bay, north-eastern Mediterranean Sea. *Turkish Journal of Fisheries and Aquatic Sciences,* ***13***(3): 541–549.

Fernandes, C., Fontaínhas-Fernandes, A., Peixoto, F. & Salgado, M. A. (2007). Bioaccumulation of heavy metals in *Liza saliens* from the Esmoriz-Paramos Coastal Lagoon, Portugal. *Ecotoxicology and Environmental Safety*, ***66***(3): 426–431.

Fernandez-Reiriz, M. J., Pastoriza, L. & Sampedro, G. (1992). Lipid changes in muscle tissue of ray (*Raja Clavata*) during processing and frozen storage. *Journal of Agricultural and Food Chemistry,* ***40***(3): 484–488.

Filiz, H. & Bilge, G. (2004). Length-weight relationships of 24 fish species from the north Aegean Sea, Turkey. *Journal of Applied Ichthyology,* ***20***(5): 431–432.

Foran, S. E., Flood, J. G. & Lewandrowski, K. B. (2003). Measurement of mercury levels in concentrated over-the-counter fish oil preparations. *Archives of Pathology & Laboratory Medicine,* ***127***(12): 1603–1605.

Gümgüm, B., Ünlü, E., Tez, Z. & Gülsün, Z. (1994). Heavy metal pollution in water, sediment and fish from the Tigris River in Turkey. *Chemosphere*, ***29***(1): 111–116.

Ichihara, K., Shibahara, A., Yamamoto, K. & Nakayama, T. (1996). An improved method for rapid analysis of the fatty acids of glycerolipids. *Lipids,* ***31***(5): 535–539.

Ismen, A. (2003). Age, growth, reproduction and food of common stingray (*Dasyatis pastinaca* L., 1758) in Iskenderun Bay, the eastern Mediterranean. *Fisheries Research,* ***60***(1): 169–176.

Jabeen, F. & Chaudhry, A. S. (2011). Chemical compositions and fatty acid profiles of three freshwater fish species. *Food Chemistry,* ***125***(3): 991–996.

Jankowska, B., Zakeś, Z., Zmijewski, T. & Szczepkowski, M. (2010). Fatty acid profile of muscles, liver and mesenteric fat in wild and reared perch (*Perca fluviatilis* L.). *Food Chemistry*, ***118***(3): 764–768.

Juresa, D. & Blanusa, M. (2003). Mercury, arsenic, lead and cadmium in fish and shellfish from the Adriatic Sea. *Food Additives & Contaminants,* ***20***(3): 241–246.

Kaur, N., Chugh, V. & Gupta, A. K. (2012). Essential fatty acids as functional components of foods: A review. *Journal of Food Science and Technology*, ***51***(10): 2289-2303.

Kadri, H., Saïdi, B., Marouani, S., Bradai, M. N. & Bouaïn, A. (2013). Food habits of the rough ray *Raja radula* (Chondrichthyes: Rajidae) from

the Gulf of Gabès (central Mediterranean Sea). *Italian Journal of Zoology,* ***80***(1): 52–59.

Mendil, D., Ünal, Ö. F., Tüzen, M. & Soylak, M. (2010). Determination of trace metals in different fish species and sediments from the River Yeşilırmak in Tokat, Turkey. *Food and Chemical Toxicology,* ***48***(5): 1383–1392.

Masoud, M. S., El-Samra, M. I. & El-Sadawy, M. M. (2007). Heavy-metal distribution and risk assessment of sediment and fish from El-Mex Bay, Alexandria, Egypt. *Chemistry and Ecology,* ***23***(3): 201–216.

Navarro-Garcia, G., Gonzalez-Filix, M. L., Marquez-Faras, F., Bringas-Alvarado, L., Prez-Velazquez, M., Montoya-Laos, J. M. & Moreno-Silva, B. (2014). Lipid content and fatty acid composition of the liver from the Rajiforms *Urotrygon chilensis*, *Urobatis halleri*, *Rhinobatos glaucostigma*, *Rhinoptera steindachneri* and *Dasyatis dipeteura* captured in Sinaloa, Mexico. *International Food Research Journal,* ***21***(1): 229–235.

Navarro-Garcia, G., Pacheco-Aguilar, R., Bringas-Alvarado, L. & Ortega-García, J. (2004). Characterization of the lipid composition and natural antioxidants in the liver oil of *Dasyatis brevis* and *Gymnura marmorata* rays. *Food Chemistry,* ***87***(1): 89–96.

Navarro-Garcia, G., Ramírez-Suárez, J. C., Cota-Quiñones, E., Márquez-Farías, F. & Bringas-Alvarado. L. (2010). Storage stability of liver oil from two ray (*Rhinoptera bonasus* and *Aetobatus narinari*) species from the Gulf of Mexico. *Food Chemistry*, ***119***(4): 1578-1583.

Navarro-Garcia, G., Ramirez-Suarez, J. C., Ortega-García, J., García-Camarena, R., Márquez-Farías, F., Santos-Valencia, J. & Bringas-Alvarado, L. (2009). Lipid composition, natural antioxidants and physicochemical characteristics in liver oil from rajiforms from the Gulf of Mexico. *Journal of the American Oil Chemists' Society,* ***86***(4): 323–328.

Olusoji, B. O. A., Anifowose, O. J. & Sodamola, M. Y. (2010). Length-weight relationships, condition factor and fecundity of the West Africa freshwater crab, *Sudanonautes africanus* (Milne-Edwards 1883), in Western Nigeria. *West African Journal of Applied Ecology*, ***16***(1): 65–74.

Ould El Kebir, M. V., Barnathan, G., Siau, Y., Miralles, J. & Gaydou, E. M. (2003). Fatty acid distribution in muscle, liver, and gonads of rays (*Dasyatis marmorata*, *Rhinobatos cemiculus*, and *Rhinoptera marginata*) from the east tropical Atlantic Ocean. *Journal of Agricultural and Food Chemistry,* ***51***(7): 1982-1947.

Ozyilmaz, A. (2016). Tocopherol, heavy metals (Cd, Pb, Cu, Fe, Mn, Zn), and fatty acid contents of thornback ray (*Raja clavata* Linnaeus, 1758) liver oil in relation to gender and origin in the Mediterranean and Black Seas). *Journal of Applied Ichthyology,* ***32***(3): 564–568.

Pal, D., Banerjee, D., Patra, T. K., Patra, A. & Ghosh, A. (1998). Liver lipids and fatty acids of the sting ray *Dasyatis bleekeri* (Blyth). *Journal of the American Oil Chemists' Society,* ***75***(10): 1373–1378.

Saglam, H. & Bascinar, N. S. (2008). Feeding ecology of thornback ray (*Raja clavata* Linnaeus, 1758) on the Turkish coast of the southeastern Black Sea. *Marine Biology Research,* ***4***(6): 451–457.

Tufan, B., Koral, S. & Köse, S. (2013). The variations in proximate chemical composition and fatty acid profile in different parts of the thornback ray (*Raja clavata*) caught from Black Sea, Turkey. *Journal of Aquatic Food Product Technology,* ***22***(1): 83–95.

Turan, H. (2007). Fatty acid profile and proximate composition of the thornback ray (*Raja clavata*, L. 1758) from the Sinop coast in the Black Sea. *Journal of FisheriesSciences.com,* ***1***(2): 97–103.

Türkmen, M., Türkmen, A. & Tepe, Y. (2014). Comparison of metal levels in different tissues of seven ray species from Antalya Bay, Mediterranean Sea. *Bulletin of Environmental Contamination and Toxicology,* ***93***(2): 159–164.

Ulbricht, T. L. V. & Southgate, D. A. T. (1991). Coronary heart disease: Seven dietary factors. *Lancet,* ***338***(8773): 985-992.

Wiktorowska-Owczarek, A., Berezińska, M. & Nowak, J. (2015). PUFAs: Structures, metabolism and functions. *Advances in Clinical and Experimental Medicine,* ***24***(6): 931–941.

Yeldan, H., Avsar, D. & Manaşirli, M. (2009). Age, growth and feeding of the common stingray (*Dasyatis pastinaca*, L., 1758) in the Cilician Coastal Basin, northeastern Mediterranean Sea. *Journal of Applied Ichthyology,* ***25***(1): 98–102.

Yılmaz, A. B., Yanar, A. & Alkan, E. N. (2017). Review of heavy metal accumulation on aquatic environment in northern east Mediterranean Sea part I: Some essential metals. *Reviews on Environmental Health,* ***32***(1-2): 119–163.

Mar. Sci. Tech. Bull. (2019) 8(1): 23-29
e–ISSN: 2147–9666
info@masteb.com

http://dergipark.gov.tr/masteb
http://www.masteb.com/
DOI: 10.33714/masteb.547103

Marine Science and Technology Bulletin

RESEARCH ARTICLE

The Reflection of Ship Demolition Prices to Construction Costs in Turkey

Abdullah Açık[1] • Esra Baran[1*]

[1] *Dokuz Eylül University, Maritime Faculty, Buca, İzmir, Turkey*

ARTICLE INFO

Article History:

Received: 30.03.2019
Received in revised form: 31.05.2019
Accepted: 17.06.2019
Available online: 20.06.2019

Keywords:
Construction cost
Demolition price
Exchange rate

ABSTRACT

The ship demolition sector is one of the major suppliers of the steel market, even though its share in the total scrap market is very small. As the sector is a supplier of the steel market, it is inevitable that the price changes will be reflected in the construction sector, which is one of the largest steel customers. In this context, it is aimed in this study to determine whether the changes in demolition prices of Turkey, which is one of the main ship demolition locations in the world, have an effect on the construction costs in the country. In order to investigate possible relationships, Turkish demolition prices and Construction Cost Index (CCI) variables are used. The dataset covers the dates between January 2015 and December 2018, and consists of 48 monthly observations. Asymmetric causality test is used to determine the causal relationship between the variables by separating the shocks they contain as positive and negative. The econometric relationship is analyzed with both the USD currency price offered by Turkish demolition businesses and the corresponding TL currency prices in order to diversify the results. According to the results, causality relation from positive shocks in USD based demolition prices to the positive shocks in construction costs index is determined. In addition, there are causalities from positive shocks in TL based demolition prices to the positive shocks in construction cost index, and from negative shocks in demolition prices to the negative shocks in the index. This situation shows that the foreign exchange rates also play an important role in shaping the costs of the construction sector.

Please cite this paper as follows:

Açık, A., Baran, E. (2019). The Reflection of Ship Demolition Prices to Construction Costs in Turkey. *Marine Science and Technology Bulletin*, 8(1): 23-29.

Introduction

The scrap sector meets some part of the demand for steel by supplying the scrapped steel to the market (Merikas et al., 2015). Products obtained from this scrapped steel are generally used as construction iron. From this point of view, it is not unreasonable to say that changes in scrap iron prices cause changes in the iron supply costs of the construction sector, which consequently cause a change in the general cost of construction.

A relatively small portion of the scrap sector is obtained from ship demolition activities (Mikelis, 2013). Ships that have completed their economic life are sent to demolition and become both an income source for shipowners and a steel source for the construction sector (Strandenes, 2010). The demolition activities are carried out in a few locations across the world such as Bangladesh, China, India, Pakistan, and Turkey, and these countries offer a specific price per tonne to attract ships. This offered price is affected by both maritime market (Mikelis, 2007; Açık and Başer, 2018a) and steel market (Mikelis,

* Corresponding author
E-mail address: abdullah.acik@deu.edu.tr (A. Açık)

2013), however these interactions are not covered by this study. In this study, the aim is to examine the causal relationship between the proposed price for demolition by Turkish demolition businesses and the construction costs in the country. For representing construction costs in Turkey, Construction Cost Index (CCI) published by TURKSTAT is used.

The relationship between the price of ship demolition and the construction cost is examined and diversified in two ways. The first one is examining with USD currency, which is the original demolition price, and the second one is examining with corresponding TL value of the original demolition price. Taking into account the possibility of losing their linearity since the financial series are exposed to many unexpected events and shocks, the relationship between variables is examined by nonlinear causality analysis in addition to the linear causality analysis. It is thought that the implementation of the two kind of analyses is functional in order to discover whether the relationship between the variables is linear and to prove the advantage of the method used. The selected nonlinear analysis is the asymmetric causality analysis, which enables to determine the causality relationship between the positive and negative shocks included by the considered variables. This feature is important since it is natural for players in the market to react differently depending on the type of shock.

No significant relationship can be obtained according to the linear causality analysis, and the linearity of the series is investigated with the Brock, Dechert and Scheinkman (BDS) test. Since the BDS test reveals that the series are not linear, the asymmetric causality test is applied. According to the results of the analyses, significant results are obtained in both cases. Positive shocks in demolition prices with USD currency are the cause of positive shocks in construction cost index. On the other hand, in the case of corresponding TL values, positive shocks in the demolition prices are the causes of positive shocks in the construction cost index, and negative shocks in the demolition prices are the causes of negative shocks in construction cost index. This situation shows that the foreign exchange rates also play an important role in shaping the costs of the construction sector as well as the international prices. Increasing shocks in USD based prices are reflected in the construction sector costs immediately, while lowering shocks are not reflected. Instead, the lowering shocks in TL based prices have led to lowering shocks in the cost of construction sector due to the drop in the exchange rates.

The related literature is evaluated in the second section of the study and the current study is positioned. The method used in the study is introduced and the reasons for its use are expressed in the third section. The relevant data set is examined and the results obtained from analyses are presented in the fourth section. The results are evaluated and several policy implications are proposed in the last section.

Literature Reviews

As mentioned by Karlis and Polemis (2016) ship demolition market literature is predominantly centered around the environmental and regulatory parts of the point. There are fairly limited and rare studies focused on the economic analysis of the sector and the factors affecting demolition sector. In summary, the main topics related to the demolition industry in the literature; the probability of a vessel to be scrapped in major demolition yards in the world and impact of several factors on that probability (Knapp et al., 2008), the relationship between international scrap price and demolition price (Kagkarakis et al., 2016), the process of ship sale for demolition (Karlis and Polemis, 2016), the relationship between freight levels and the amount of vessel sent to the demolition (Açık and Başer, 2017), the impact of supply side on the price formation in demolition industry (Kagkarakis, 2017), the relationship between the demolition price and the freight level in the dry bulk market (Açık and Başer, 2018a), market efficiency in ship demolition prices (Açık and Başer, 2018b), ship demolition decisions of individual shipowners in different market conditions (Yin and Fan, 2018). Also, some evaluations are made about ship demolition market through various statistical data in some studies (Buxton, 1991; Mikelis, 2007; Mikelis, 2013).

The study of Knapp et al. (2008) provides useful insights into the dynamics of the ship demolition market by applying econometric analysis with a comprehensive data set covering 29-year period and collected from several sources. The findings conclude a negative relationship with earnings which means an increase in earnings decreases the probability of a ship being demolished, and a positive relationship with demolition prices which means an increase in the demolition price will lead to a higher probability of ships being scrapped.

Kagkarakis et al. (2016) have investigated the causal relationship between international steel-scrap prices and ship demolition prices. Their findings have resulted that the ship demolition price is also determined by other market conditions such as the international steel-scrap trade. The steel-scrap imports in the ship demolition regions are quite higher than the volume of scrap-metal obtained from ship demolition. They have also suggested that the signals provided by the global steel-scrap prices to the ship demolition market can be taken into consideration by shipowners and practitioners.

Karlis and Polemis (2016) have analyzed the ship sale process for demolition by focusing on the monetary flows of the ships sale activity. They have stated that the ship sale decision for demolition market is oriented by some factors, for instance the state of the market cycle, which is considered to be the most important one. The ship sale decision of the shipowner will be affected by the offered ship scrapping price.

In a study conducted by Açık and Başer (2017), the relationship between the freight rates and the amount of vessel sent to the scrapping is investigated through correlation and regression analysis. In theory, the decline of revenues in the market causes the operational activities of old and obsolete ships to be unsustainable, therefore when the freight rates fall, there is an increase in the amount of vessel going to scrapping. As a result of analyses carried out by the authors, they confirm the negative relationship between the freight rates and the amount of ship sent to the scrapping.

In the study of Kagkarakis (2017) the effects of both the supply and the demand factors on the ship-demolition price formation has been investigated by the vector autoregressive model method in the crude tanker and the bulk carrier markets. The findings of the study have

showed that the supply side factors have limited impact on the price formation in the demolition industry.

In another study conducted by Açık and Başer (2018a), the relationship between the scrap prices and the freight rates has been examined. The increase in freight rates implies an economic recovery, as the demand for transportation activities has increased. In addition, as mentioned in the previous studies by the same authors, the increase in freight rates cause a decrease in the amount of vessel sent to the demolition (Açık and Başer, 2017). Increased steel demand caused by the economic recovery and the shortage of ships in the demolition yards due to the buoyant freight market conditions may cause an increase in the offered demolition prices. In the results of the analyses carried out in this context, the positive relationship between freight rates and demolition prices is confirmed by the authors.

Açık and Başer (2018b) have investigated the validity of the weak form Efficient Market Hypothesis in the demolition prices. Being efficient in the weak form means that the prices do not have a relationship with their historical values and they move randomly. However, some demolition market factors such as its small share in the general scrap industry (Mikelis, 2013), its close relationship with general scrap prices (Mikelis, 2007; Açık and Başer 2018b), its relationship with freight market conditions (Buxton, 1991; Açık and Başer, 2017), its limited locations in the word, and its sensitivity to steel industry demand (Kagkarakis et al., 2016) are said to be prevent the prices from moving randomly. The authors have concluded that the demolition prices of five major demolition locations (Bangladesh, China, India, Pakistan, and Turkey) are not efficient in the weak form as a result of the BDS test.

The individual shipowners' ship demolition decisions and their behavioral changes after the financial crisis period have been analyzed by Yin and Fan (2018). The findings of the survival analysis models (the one period before the financial crisis in 2008 and one after) have indicated that while the main actors of ship demolition market are the shipowners from developed countries before the financial crisis, more shipowners from developing countries started to get involved after the crisis period.

One of the main customers of the steel market is the construction industry. Although the share of ship scrap remains small in the steel industry, it is not a poor opinion to think that it affects the general market. Therefore, it is likely that there is a relationship between ship demolition prices and construction costs. However, as can be seen from the literature reviewed, no studies that examined this possible relationship econometrically have been found. In this regard, this study offers an original contribution to the literature by examining the relationship by the case of Turkish industries. Moreover, another important point that increases the originality of the study is the method used. Due to the partly complex nature of the ship demolition market affected by both the maritime market and the steel market, it is difficult to establish linear relations. In this context, the asymmetric causality test, which provides the opportunity to examine the relationships in a nonlinear manner by separating the shocks in the variables as positive and negative, strengthens the findings of the study.

Methodology

In accordance with the purpose of the study, used methods respectively are standard linear causality analysis, BDS test and asymmetric causality analysis. Standard linear causality analysis is used both to determine the direction of the relationship between variables and to show the possible insufficiency of linear methods in determination causal relationships in the maritime markets. The BDS test is used to examine whether the series are linear or not, in addition to the information obtained from distributions of the variables. Finally, the asymmetric causality test is used to examine the possible nonlinear relationship between the variables by separating the shocks as negative and positive.

The most basic method of investigating causality relationships between variables is the standard linear causality analysis developed by Granger (1969). This method tests the causality relationship between the two variables by investigating whether the past values of first variable can explain the current and future values of the second one (Yu et al., 2015). In other words, the Granger causality matters if there is a correlation between the present value of the first variable and the past values of the second one (Chiou-Wei, 2008). However, studies conducted in later periods have showed that linear methods may be insufficient to detect non-linear relationships (Adıgüzel et al., 2013; Bal and Rath, 2015; Kumar, 2017). This deficiency constitutes an important obstacle, especially considering that the economic and financial series in the today's globalized world are constantly exposed to unexpected shocks and crises.

The standard causality test can be used in a healthy way by verifying that the structure of the series is linear. In order to test the linearity structure, the distribution of the series can be examined, or some additional tests can be used. One of the most common methods used for investigating the nonlinearity is the BDS test developed by Brock, Dechert and Scheinkman (1987). It is applied to the residuals that are separated from an estimated equation, and it checks whether the residuals are independent and identically distributed. The null hypothesis of this test indicates that the series conform to these assumptions (Brock et al., 1996), and the rejection of the null hypothesis indicates that the residues contain some hidden and nonlinear structure. The rejection of the null hypothesis implies that the nonlinear Granger causality test is more appropriate than the linear one (Lim and Ho, 2013).

The nonlinear causality test used in this study is the asymmetrical causality analysis developed by Hatemi-J (2012a). The advantage of this method is that it can separate the shocks included in the variables as positive and negative ones, and investigate the causal relationships between them in four possible combinations; (i) from positive shocks to positive shocks, (ii) from positive shocks to negative shocks, (iii) from negative shocks to negative shocks, and lastly, (iv) from negative shocks to positive shocks. The test constructs cumulative sums of positive and negative shocks in order to determine causal relationships between them (Tugcu and Topcu, 2018), and thus causal impacts of positive shocks and negative shocks can be separated (Shahbaz et al., 2017). This feature is very useful since asymmetric positive and negative shocks can produce different impacts (Hatemi-J, 2012b). In

addition, players in the market may react differently depending on the type of shock they are exposed to (Hatemi-J, 2012a).

Some initial values must be determined before the asymmetric causality test is applied. Firstly, since this test follows a Toda and Yamamoto (1995) process, it is necessary to determine the appropriate degree of integration (Umar and Dahalan, 2016). Various unit root tests can be used for this, and if there is a unit root in the series, an extra lag is added to the unrestricted VAR models (Hatemi-J and Uddin, 2012). In this study, the augmented Dickey-Fuller (ADF) unit root test developed by Dickey and Fuller (1979) is used. Another value that must be determined before the analysis is the type of information criterion that allows to identify the best model. In this study, one of the most commonly used criteria, Akaike Information Criteria (AIC) is used in both before the implementation of BDS test and asymmetric causality test. The other last two values are the maximum number of lags and the number of bootstrap simulations.

Eviews 10 and GAUSS 10 econometric software packages are used in the analysis process. The former is used in the unit root test, the standard Granger causality test, ARIMA estimation and BDS tests while the latter is used in the asymmetric causality test. In the next section, the process explained here is followed and the results of the analysis are presented.

Results

Descriptive statistics of the series are presented in Table 1. The dataset covers the dates between January 2015 and December 2018, and consists of 48 monthly observations. As the demolition prices are obtained in US dollar currency, the statistics for the USD / TL parity used to convert them to TL are also included in the table. The term of the demolition prices refers to the US dollars per Light Displacement Tonnage (LDT) that offered to old or obsolete vessels by the ship demolition operations. The measure of LDT is an indication of the amount of steel contents of the vessels. The total demolition value of the ship is determined by multiplying the offered demolition price by LDT (Allum, 2013).

The Skewness and Kurtosis values in the descriptive statistics also provide information about the types of shock that the variables are mostly exposed. If the value of Kurtosis higher than 3, the sign of Skewness often indicates the type of shocks (news) that is mostly exposed to. When the values of the variables transformed into the return series are examined, it can be seen that CCI and USD variables have positive skewness values, while both other Demo variables have negative values. These results indicate that the construction cost index and the USD / TL parity are more exposed to positive shocks in the covered period. On the other hand, both types of demolition prices are more exposed to negative shocks in the covered period.

It is also possible to obtain information about the linearity of the series from the descriptive statistics. The lack of normal distribution of the series may indicate that they are not linear (Shahbaz et al., 2017) since the linear structures of the series exposed to too many unexpected shocks are deteriorated. The determination of the normal distribution is determined by Jarque-Bera test, and the null hypothesis of this test indicates that the series have a normal distribution. When JB probabilities of return series are examined, the null hypothesis is rejected in all variables, and there is strong evidence that the series are not linear. This information is important because the asymmetric causality test is a nonlinear method. In order to strengthen this information obtained from descriptive statistics, the Brock, Dechert and Scheinkman (BDS) test is also applied to the series in the further process.

Table 1. Descriptive statistics of the data

Values	CCI	DEMO	USD	DEM. TL	ΔLNCCI	ΔLNDEM	ΔLNUSD	ΔLNDEM. TL
Mean	126.1	224.4	3.55	816.3	0.01	-0.00	0.01	0.01
Median	121.7	231.3	3.48	709.6	0.00	0.00	0.01	0.02
Maximum	182.8	300	6.37	1552	0.07	0.16	0.18	0.15
Minimum	97.1	148	2.33	435.1	-0.03	-0.24	-0.08	-0.19
Std. Dev.	25.2	44.1	0.93	324.0	0.01	0.08	0.04	0.08
Skewness	0.81	-0.04	1.31	0.74	1.09	-0.77	0.83	-0.84
Kurtosis	2.58	1.70	4.20	2.35	4.95	3.68	5.73	3.72
Jarque-Bera	5.62	3.38	16.7	5.20	16.9	5.58	20.0	6.58
Probability	0.06	0.18	0.00	0.07	0.00	0.06	0.00	0.03
Observations	48	48	48	48	47	47	47	47

Source: TCMB (2019); TUIK (2019); Athenian Shipbrokers (2019)

Augmented Dickey-Fuller (1979) test is applied to all series for stationarity control, and the results are presented in Table 2. The application of this test is essential for 3 reasons; (i) the series must be stationary for the implementation of the standard Granger causality test; (ii) the series must be stationary in order to estimate the ARIMA models and carry out the BDS test on their residuals; (iii) there is no requirement for stationarity of the variables in the asymmetric causality test, however the maximum degree of integration must be known. According to the results of these tests, all variables become stationary when the first differences are taken. This stationarity information also indicates the maximum degree of integration in the asymmetric causality test.

Table 2. Augmented Dickey-Fuller unit root test results

Variable	Level		First Difference	
	Intercept	Trend and Intercept	Intercept	Trend and Intercept
Construction Cost Index	0.789	-2.300	-4.920***	-4.933***
Turkish Demolition Prices ($)	-1.765	-3.358*	-2.798*	-2.876***
Turkish Demolition Prices (TL)	0.053	-2.956	-6.557***	-6.514***

Note: Critical values: -2.560 for *10%, -2.92 for **5%, -3.57 for ***1% at Intercept; -3.18 for *10%, -3.51 for **5%, -4.17 for ***1% at Trend and Intercept.

In addition, the causality relationship between variables is also tested by the linear method. The analyses are carried out with stationary variables in both US dollar and TL basis and the results are presented in Table 3. The optimum lags for both tests are determined as 1 according to AIC, SC and HQ information criteria. According to the results obtained, the null hypotheses are rejected in all cases, and neither the USD nor the TL-based causality relationships can be determined. This may be considered to indicate the insufficiency of the linear method to detect nonlinear relationships. In this respect, BDS test, which is commonly used in determination of the non-linearity, is carried out.

Table 3. Standard Granger causality analysis

Null Hypothesis:	Obs.	F-Statistic	Prob.
ΔLNDEMO does not Granger Cause ΔLNCCI	46	0.20123	0.6560
ΔLNCCI does not Granger Cause ΔLNDEMO		0.00246	0.9607
ΔLNDEMOTL does not Granger Cause ΔLNCCI	46	0.59958	0.4430
ΔLNCCI does not Granger Cause ΔLNDEMOTL		0.00628	0.9372

First of all, all the variables are converted into financial return series by using $R_i = ln_i - ln_{i-1}$. In order to implement the BDS test in the most appropriate way, the deterministic parts of the data must be separated firstly, since the rest of the data after this process is the variance of the series. To separate the deterministic parts, the most appropriate ARIMA model is determined for each variable through lowest AIC (Akaike Information Criteria) values. Then the best models are estimated, and the residuals of the models are separated. Finally, BDS test is applied to these residuals for 6 dimensions in order to determine non-linear structures if any. The null hypothesis of this test indicates that the series contains a non-linear structure, and even if the null hypothesis is rejected in one of the dimensions, it indicates that there is a nonlinear structure in the series. The same process is followed for each variable using the automatic ARIMA forecasting function in an econometric software.

Firstly, the most suitable model for the Construction Cost Index (CCI) variable is determined as the model of ARMA (1, 0) with -5.41 AIC value. Then, after the model is estimated, the residuals of the model are subjected to the BDS test and the results are presented in Table 4. According to the results obtained, the null hypotheses in the second and sixth dimensions are rejected and the nonlinear structure in the series is confirmed. Secondly, the most suitable model for Demolition Price in US dollar currency (DEMO) variable determined as the model of ARIMA (5, 5) with -2.21 AIC value. According to the results of the BDS test applied to the residuals, the null hypotheses are rejected in the second, third and fifth dimensions. These results confirm the nonlinear structure in this variable. Finally, the most suitable model for Demolition Price in TL currency (DEMOTL) is determined as ARIMA (3, 1) model with -2.13 AIC value. According to the BDS test applied to the residuals, the null hypotheses are rejected in the second, fourth and sixth dimensions. Consequently, all variables contain nonlinear structures, which imply the applicability of the nonlinear asymmetric causality test.

Table 4. BDS independence test results

Dimension	CCI Prob.	Demo USD Prob.	Demo TL Prob.
2	0.0274**	0.0132**	0.0905*
3	0.2596	0.0444**	0.1056
4	0.5452	0.1081	0.0587*
5	0.4430	0.0872*	0.1199
6	0.0109**	0.3913	0.0445**

Then the process of the implementation of the asymmetric causality test begins. Some initial values must be determined before this test is performed, which are the maximum degree of integration (dmax), the maximum lags value, the type of information criterion to choose the most suitable model, and the maximum number of the bootstrap simulation. The dmax value is the maximum difference that must be taken in order to make both variables used in the analysis stationary. Unit root tests are used for the determination of this value, and according to the ADF unit root test results presented in Table 1, all variables become stationary when the first differences are taken. That is, the maximum degree of integration is determined as 1. The maximum number of lags, which is the other value to be determined, is set to 4 since the number of the observations in the analysis is small and the data frequency is monthly. The type of information criteria used to select the most suitable model is determined as Akaike Information Criteria (AIC), which is one of the most widely used one. Lastly, the maximum number of bootstrap simulations is selected as 1000. Then, the asymmetric causality test is applied.

The results of the asymmetric causality test are presented in Table 5. According to the results, while one significant causality has been determined from the USD based demolition price to the Construction Cost Index, two significant causal relationships have been determined from the TL based demolition price. The positive shocks in the USD Demo variable are the cause of positive shocks in the CCI variable. Increasing shocks that the price of the demolition is exposed to are the cause of the increasing shocks of construction costs. However, there is no relationship between negative shocks. On the other hand, the positive shocks in the TR Demo variable are the cause of positive shocks in the CCI variable, and negative shocks in the TR Demo variable are the cause of negative shocks in the CCI variable. Unlike the USD-based price, lowering shocks in the TR price are the cause of negative shocks in the construction cost.

Table 5. Asymmetric causality test results

Values		USD Demo → Construction				TR Demo → Construction			
		D^+C^+	D^+C^-	D^-C^-	D^-C^+	D^+C^+	D^+C^-	D^-C^-	D^-C^+
Optimal Lag; VAR(p)		4	1	2	1	4	1	3	1
Additional Lags		1	1	1	1	1	1	1	1
Test Stat (MWALD)		7.97	0.04	0.69	0.28	14.0	0.46	8.12	0.24
Asym. chi-sq. p-value		0.09*	0.83	0.70	0.59	0.00***	0.49	0.04**	0.62
Critical Val.	1%	34.2	11.2	17.4	10.2	35.0	14.5	31.0	13.3
	5%	16.5	5.04	10.5	5.50	17.0	5.39	17.1	5.47
	10%	11.6	3.14	6.99	1.05	11.4	3.04	11.3	3.17

Note: Significance levels: *10%, **5%, ***1%.

Conclusion

The impact of Turkish demolition prices, which is one of the major ship demolition countries in the world, on construction costs have been investigated through Construction Cost Index. Although the share of ship scrap in the total steel market is quite small, it is likely that there will be a significant relationship as the steel from the ship demolition is mostly used in the domestic market. In addition, as the demolition price is affected by both the maritime market and the steel market, it is likely to follow a parallel line with general steel prices in the market. In this respect, construction cost changes since the general steel prices are also associated with demolition prices. However, as the subject also has a maritime side, the relationship is not clear and becomes partially complicated. Especially, developments in the freight market affect the number of ships sent to the demolition (Açık and Başer, 2017) and demolition prices (Açık and Başer, 2018) consequently. Taking into account all of these, the relationship between demolition price and construction cost is likely to be non-linear.

Although the main focus of the study is the asymmetric causality method, standard linear causality analysis is also applied to show that the relationship between the variables is not linear. Following the reaching of insignificant results from the linear method, the nonlinearity is tested, and asymmetrical causality analysis is applied. In the USD based prices, only one significant relationship is obtained from four possible combinations, and this proves the accuracy of selecting the method used. Only the positive shocks in the demolition price are determined as the cause of the positive shocks in the Construction Cost Index. However, a negative response to a negative impact in the linear method is also a strong possibility. On the other hand, in the TL based prices, causality from negative shocks in demolition prices to negative shocks in construction costs have been spotted, in addition to the causality spotted between positive shocks as in the case of previous currency.

The double causal relations from the TL based prices are probably due to the imported materials that are included in the construction cost basket. Since TL based demolition price is negatively affected by the decrease in the exchange rate as well as the decrease in the USD based demolition price, downward movements in the construction cost occur when the TL based price decreases. Accordingly, positive shocks in the demolition prices cause positive shocks in the construction cost index, which may be the result of both other kind of imported materials and the price of steel.

It is hoped that the findings obtained for the construction sector provide partial useful results for risk minimization and future foresight. Especially the positive shocks in scrap prices may have a positive impact on construction costs, which may directly affect the profitability of firms in the sector. In this context, considering the general parallel movement of the demolition prices with the developments in the freight market, it is suggested that firms in the construction sector should observe the trends in the freight market while pricing for their products, as the profitability of the firms can be affected significantly due to the fluctuations in demolition prices in the period between construction and sales.

In the literature, the interaction of demolition prices with the steel market is partly examined, however, the impact on construction costs is not examined by this approach. In this respect, it is thought that the originality of this study is related both to the unique subject and to the use of asymmetric causality method for the first time.

As a constraint to the study, only the Construction Cost Index data starting from 2015 could be reached. Better results can be obtained with a longer time interval. Similar relations can also be tested for other major demolition countries and more generalizable results can be obtained. In addition, Construction Cost Index can be examined separately according to the possible sub-indices, and the relationship between the steel-based index and demolition price can be considered in a more concrete manner.

Conflict of Interest

The authors declare that there is no conflict of interest.

References

Açık, A. & Başer, S. Ö. (2018a). The relationship between freight rates and demolition prices. *Journal of International Trade and Economic Researches*, ***2***(1): 16-32.

Açık, A. & Başer, S. Ö. (2018b). Market efficiency in ship demolition prices. *Proceedings of the International Conference on Empirical Economics and Social Sciences*, Bandırma, Turkey, pp. 780-792.

Açık, A. & Başer, S. Ö. (2017). The relationship between freight revenues and vessel disposal decisions. *Journal of Research in Economics, Politics & Finance*, ***2***(2): 96-112.

Allum, S. (2013). Residual value insurance in the maritime sector. In: *Intellectual Property Valuation and Innovation* (pp. 135-156). Routledge.

Adıgüzel, U., Bayat, T., Kayhan, S. & Nazlıoğlu, Ş. (2013). Oil prices and exchange rates in Brazil, India and Turkey: Time and frequency domain causality analysis. *Research Journal of Politics, Economics and Management,* ***1***(1): 49-73.

Athenian Shipbrokers S. A. (2019). Demolition prices. Retrieved in February 10, 2019 from https://hellenicshippingnews.com/.

Bal, D. P. & Rath, B. N. (2015). Nonlinear causality between crude oil price and exchange rate: A comparative study of China and India. *Energy Economics*, ***51***: 149-156.

Brock, W., Dechert, D., Sheinkman, J. & LeBaron, B. (1996). A test for independence based on the correlation dimension. *Econometric Reviews*, ***15***(3): 197–235.

Brock, W., Dechect, W. & Scheinkman, J. (1987). A test for independence based on the correlation dimension. Working Paper. Department of Economics, University of Wisconsin, Madison.

Chiou-Wei, S. Z., Chen, C. F. & Zhu, Z. (2008). Economic growth and energy consumption revisited—Evidence from linear and nonlinear Granger causality. *Energy Economics*, ***30(***6): 3063-3076.

Dickey, D. A. & Fuller, W. A. (1979). Distribution of the estimators for autoregressive time series with a unit root. *Journal of the American Statistical Association*, ***74(***366a): 427-431.

Granger, C. W. (1969). Investigating causal relations by econometric models and cross-spectral methods. *Econometrica: Journal of the Econometric Society*, ***37***(3): 424-438.

Hatemi-J, A. (2012a). Asymmetric causality tests with an application. *Empirical Economics*, ***43***(1): 447-456.

Hatemi-J, A. (2012b). Is the UAE stock market integrated with the USA stock market? New evidence from asymmetric causality testing. *Research in International Business and Finance*, ***26***(2): 273-280.

Hatemi-J, A. & Uddin, G. S. (2012). Is the causal nexus of energy utilization and economic growth asymmetric in the US?. *Economic Systems*, ***36***(3): 461-469.

Kagkarakis, N. (2017). The effect of vessel supply on ship-demolition prices. *Eurasian Journal of Economics and Finance*, ***5***(1): 78-94.

Kagkarakis, N. D., Merikas, A. G. & Merika, A. (2016). Modelling and forecasting the demolition market in shipping. *Maritime Policy & Management*, ***43***(8): 1021-1035.

Karlis, T. & Polemis, D. (2016). Ship demolition activity: A monetary flow process approach. *Pomorstvo*, ***30***(2): 128-132.

Knapp, S., Kumar, S. N. & Remijn, A. B. (2008). Econometric analysis of the ship demolition market. *Marine Policy*, ***32***(6): 1023-1036.

Kumar, S. (2017). On the nonlinear relation between crude oil and gold. *Resources Policy*, ***51***: 219-224.

Lim, S. Y. & Ho, C. M. (2013). Nonlinearity in ASEAN-5 export-led growth model: Empirical evidence from nonparametric approach. *Economic Modelling*, ***32***: 136-145.

Merikas, A., Merika, A. & Sharma, A. (2015, January). Exploring price formation in the global ship demolition market. In 2015 Annual Meetings.

Mikelis, N. E. (2007). A statistical overview of ship recycling. *Paper Presented at the International Symposium on Maritime Safety, Security and Environmental Protection*, Athens, Greece.

Mikelis, N. E. (2013). Ship recycling markets and the impact of the Hong Kong Convention. *Paper Presented at the International Conference on Ship Recycling*, Malmo, Sweden.

Shahbaz, M., Van Hoang, T. H., Mahalik, M. K. & Roubaud, D. (2017). Energy consumption, financial development and economic growth in India: New evidence from a nonlinear and asymmetric analysis. *Energy Economics*, ***63***: 199-212.

Strandenes, S. P. (2010). Economics of the Markets for Ships, p. 217–234. In: Grammenos, C. (Eds.), The handbook of maritime economics and business. 2nd ed. London, UK: Lloyd's List. 1096p.

TCMB (2019). Exchange rates. Retrieved in February 10, 2019 from https://evds2.tcmb.gov.tr/index.php?/evds/serieMarket/#collapse_2.

Toda, H. Y. & Yamamoto, T. (1995). Statistical inference in vector autoregressions with possibly integrated processes. *Journal of Econometrics*, ***66***: 225–250.

Tugcu, C. T. & Topcu, M. (2018). Total, renewable and non-renewable energy consumption and economic growth: Revisiting the issue with an asymmetric point of view. *Energy*, ***152***: 64-74.

TUIK (2019). Construction Cost Index. Retrieved in February 10, 2019 from http://tuik.gov.tr/PreTablo.do?alt_id=1077.

Umar, M. & Dahalan, J. (2016). An application of asymmetric Toda-Yamamoto causality on exchange rate-inflation differentials in emerging economies. *International Journal of Economics and Financial Issues,* ***6***(2): 420-426.

Yin, J. & Fan, L. (2018). Survival analysis of the world ship demolition market. *Transport Policy*, ***63***: 141-156.

Mar. Sci. Tech. Bull. (2019) 8(1): 30–35
e–ISSN: 2147–9666
info@masteb.com

http://dergipark.gov.tr/masteb
http://www.masteb.com/
DOI: 10.33714/masteb.582223

Marine Science and Technology Bulletin

RESEARCH ARTICLE

Identification of Mislabelling in Frozen Fish Fillets Based on DNA Barcoding Analysis

Evren Koban Baştanlar[1*]

[1] *Ege University, Faculty of Science, Department of Biology, 35100, Bornova, İzmir, Turkey*

ARTICLE INFO

Article History:

Received: 25.06.2019
Received in revised form: 28.06.2019
Accepted: 29.06.2019
Available online: 30.06.2019

Keywords:
DNA barcoding
COI
Fish fillet
Mislabelling
Species substitution

ABSTRACT

A number of studies have shown that mislabelling and species substitutions in fish products are very common worldwide. This fraud has two major aspects: economics and health. Moreover, poor trading, and neglecting the species conservation status are growing threats for fish stocks. First the type and extend of this fraud in fish must be detected in order to take proper actions. As some markers (e.g. protein analysis and morphological features) can fail, DNA markers, especially sequencing of cytochrome oxidase I gene (or DNA barcoding), is becoming a more widely preferred methodology for species identification. In this study, DNA barcoding technique was employed to confirm the species names written on the product packages of fish fillets purchased from the market. The fillets were labeled as Nile tilapia (*Oreochromis niloticus*). Among the 15 fillet samples analyzed, only 4 of them were labeled correctly. Seven (47%) of them were found to originate from pangasius (*Pangasianodon hypophthalmus*) and three of them were found to originate from a different tilapia species (*Oreochromis mossambicus*). This paper revealed a significant mislabelling of frozen fish fillets in Turkey. Customers are making informed decisions based on many reasons (like health issues or palate) and they have the right to eat what they think they are paying for. The results indicate the necessity for taking immediate actions and regulations against fraud in food items to sustain food quality and safety.

Please cite this paper as follows:

Koban Baştanlar, E. (2019). Identification of Mislabelling in Frozen Fish Fillets Based on DNA Barcoding Analysis. *Marine Science and Technology Bulletin*, 8(1): 30–35.

Introduction

There is an increasing awareness in the world against fraud, mislabelling and species substitutions in food items due to health and safety problems as well as economic issues. These issues interfere with the traceability in the production chain as well as with the applications of national and international regulations. Fish are an important component of the present biodiversity with more than 30000 species existing worldwide. They are an important protein source in the human diet and they possess direct economic value. Like other food items, mislabelling and species substitutions are also major concerns in the fishery products market (FAO, 2018a). In general, substitution and mislabelling rates vary with the species and whether the product is processed or not. Moreover, the rates can be dependent on the countries, like France having one of the lowest mislabelling/substitution rates reported (Bénard-Capelle et al., 2015).

* Corresponding author
E-mail address: evrenkoban@yahoo.com (E. Koban Baştanlar)

Today, the food industry and consumers are largely focused on food safety, quality and sustainability (Di Pinto et al., 2015). Accurate labeling of domestic and imported seafood; reporting the true origin, content, and the species contained within the product are very important both for the consumer and the seller companies in order to prevent possible economic losses as well as health problems, having allergic reactions being the most important as it can be life-threatening.

Misidentifications are often made in differentiating between the species with similar morphological characteristics and in the nomenclature of species with different names for the same local name or for the same species (Cawthorn et al., 2012). Since fish meat is a perishable food, it is a common strategy filleting its meat for fish trade (Staffen et al., 2017). However, most of the morphological features used in the identification of fish species during filleting may be lost during this process. Di Pinto et al. (2013) stated that in trading fish products, aquaculture products with low economic value can be sold, in whole or in part, substituting higher quality products. For example, it has been reported in Iran that, catfish fillets can be sold instead of sturgeon fillets (Changizi et al., 2013). This is an important issue from the economic, health and food safety aspects.

There are different markers and methods used in species identification and authentication based on morphology, proteins, and DNA. Although morphological characters can be used for species identification (Strauss and Bond, 1990), they can be misleading/uninformative in discriminating especially between closely related species. Furthermore, they become useless when it comes to processed food as the characters are lost. Protein markers used in identification can be of considerable value in certain instances (Rehbein, 1990; Hubalkova et al., 2007; Asensio et al., 2008). However, like morphological characters, protein analyses can fail species identification, too. Because, proteins start losing their biological activity once the animal is dead, and they denature once they are subjected to heat. As accurate identification of fish fillets based on morphologic or allozyme markers is neither easy nor feasible, employing DNA based molecular markers for accurate identification and regular inspection of fillet products is inevitable (Smith et al., 2008).

DNA sequencing analysis is one of the most widely used molecular marker in species identification for the last two decades. But; different laboratories may prefer different DNA regions for the same taxonomic groups, or different markers are used for different taxonomic groups. In this case, conducting comparative analyses of DNA sequences within and across species cannot be carried out. In order to overcome these problems, Hebert et al. (2003) indicated that a single gene sequence would be sufficient to differentiate all or at least a large majority of animal species. For this purpose, they suggested employing the mitochondrial DNA (mtDNA) cytochrome oxidase gene subunit I (COI) as a universal biological identification system for animals. In this methodology, based on the partial sequence of the mtDNA COI region, each species is represented by a specific sequence and the sequences of individuals of the same species form a cluster. These DNA sequences are compared to databases to assign the individual sample of interest to corresponding species. This resembles the barcoding system used in stores for tracking the trade items. That is why this system is called "DNA Barcoding". Since it has been first proposed by Hebert et al. (2003), the mtDNA COI gene has been used extensively in the determination of the species belonging to a sample of unknown origin, the determination of new sequences of species and the determination of whether or not a new species of unknown origin. It has been reported that this partial nucleotide sequence analysis of COI region in species identification has a discrimination power of 98% in marine fish and 93% in freshwater fish (Ward et al., 2009).

Currently, about 40% of the total production of aquatic products is met from aquaculture, worldwide. It is reported that aquaculture production (fish, crustaceans and mollusks) in the world was 170.35 million tons in 2015 and 76.4 million tons of this production was obtained through aquaculture (FAO, 2018b), but in 1980 aquaculture was reported to be only 4.7 million tons (FAO, 2010). The estimated amount of products obtained from aquaculture by 2030 is expected to reach or exceed the production from capture fisheries (World Bank, 2013). According to TUIK data (TurkStat, 2018), Turkey has imported 82074 tons of aquatic products in 2016, 100444 tons in 2017 and 98314 tons in 2018. Among these products, imported frozen fish fillets in 2018, which is approximately 5836 tons, comprises about 6% of the total imported products (TurkStat, 2018). Nile tilapia (*Oreochromis niloticus*) is one of the imported freshwater fish species in Turkey, as fish fillets. TUIK have reported that 400 tons (~7%) of fish fillets imported in 2018 were Nile tilapia. This fish is also known as aquatic chicken (Maclean, 1984) and its production is increasing sharply in each year throughout the world (Özcan-Gökçek et al., 2012).

In the present study, we aimed at testing the accuracy of the species declarations on the package of tilapia (*O. niloticus*) products sold as fillets in the markets by using DNA barcoding method, which is accepted as a universal method in species identification.

Material and Methods

Fifteen commercially packed fish fillets were purchased from three different supermarkets, which were labeled as *O. niloticus* as the species name (Figure 1). The fillets were taken to Ege University Molecular Biology Laboratory. Approximately 100 mg of muscle tissue samples were taken from each fillet and transferred into 2 ml eppendorf tubes. Both the fillets and the tissue samples were stored at -20°C.

Figure 1. Fillet samples purchased from the supermarkets.

For the laboratory analysis, first DNAs were isolated from each tissue sample using a column-based DNA purification kit (EURX,

Molecular Biology Products). This kit was preferred because it was suitable to isolate DNA from fish muscle tissue providing high-quality DNA with repeatable results. Then, the quality and quantity of DNA samples were measured by MAESTROGEN™ spectrophotometer. In addition, the agarose gel (0.5% TBE) electrophoresis method was used to check whether the quality and quantity of DNA samples were suitable for the DNA analysis. Since all the extracted DNA samples were found to be of good quality, they were all used in the following PCR amplification reactions. For PCR amplification of the mtDNA COI gene region, primers listed in Ward et al. (2005) were used (FishF2: 5'-TCGACTAATCATAAAGATATCGGCAC-3'; FishR1:5'-TAGACTTCTGGGTGGCCAAAGAATCA-3'). The PCR reactions were performed on Applied Biosystems™ brand SimpliAmp™ thermal cycling device. The total volume of the reaction mixture was 25 µl; which contained 50 ng genomic DNA, 1X *Taq* buffer, 5 pmol from each primer, 2 mM $MgCl_2$, 0,2 mM dNTPs, 0.8 unit *Taq* DNA polymerase and ultra pure water. The cycling protocol was as follows: 1 cycle of initial denaturation at 95°C for 3 min, followed by 35 cycles at 94°C for 45 s, 54°C for 45 s, and 72°C for 60s, which then followed by the final extension at 72°C for 5 min. When performing PCR amplification, negative control without template DNA was used to check for possible contamination in every PCR reaction.

PCR amplified products were analyzed by electrophoresis on 1.5% (w/v) agarose (Sigma A5093) gel in 0.5x TBE buffer (0.089 M Tris, 0.089 M boric acid, 0.002 M EDTA, pH 8.0) and stained with SafeView DNA Stain (5 uL/100 mL) (GeneMark, Taiwan). A GeneRuler™ 100 bp DNA Ladder Plus (MBI Fermentas,Vilnius, Lithuania) was used as the molecular weight marker. Image acquisition was performed using Vilber Lourmat transilluminator. All the amplicons were about 700 bp in length as expected (Figure 2).

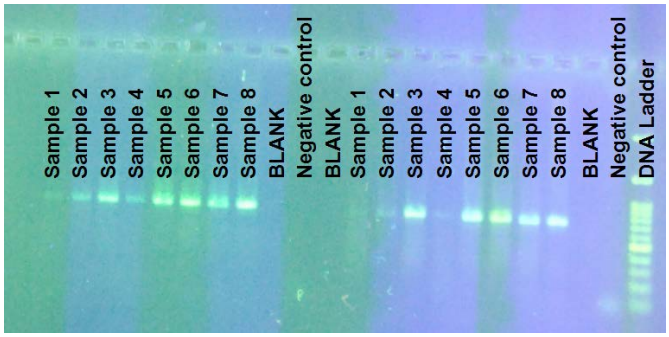

Figure 2. Imaging of the result of PCR amplification of mtDNA COI gene region of eight fish fillet samples by agarose gel electrophoresis method

Having checked the PCR products by agarose gel electrophoresis, the amplicons were transferred to LetgenBio Ltd. for bidirectional sequencing using the PCR primers given above (Ward et al., 2005). The company performs Sanger sequencing reactions using BigDye™ (Applied Biosytems™) and uses capillary-based automatic DNA Analyzers (ABI DNA Analyzer) for collecting the chromatograms.

After receiving the chromatogram results from the LetgenBio Ltd., first, they were all checked by using ChromasPro software (ChromasPro Version 2.1.8, Technelysium Pty. Ltd., Australia) for their quality. Then the chromatograms of forward and reverse sequences for each sample were aligned forming contigs. After analysis of the contigs, consensus sequences were exported in Fasta format for each sample for data analysis. The generated sequences were all subjected to BLASTn analysis at NCBI (https://blast.ncbi.nlm.nih.gov/Blast.cgi) to compare the identity of generated DNA barcodes to previously deposited sequences in order to assign the DNA samples of the study to appropriate species.

Taking the BLAST results into consideration, reference sequences were selected from the NCBI database; which are: KU565839 *Oreochromis mossambicus*, DQ426667 *Oreochromis niloticus*, LC052672 *Oreochromis niloticus*, and KR080263 *Pangasianodon hypophthalmus*. Afterward, project samples and reference samples were analyzed to find the best nucleotide substitution model using the module implemented in the MEGA 7 version (Kumar et al., 2016). The best model turned out to be HKY (Hasegawa et al., 1985) with zero gamma distribution. Finally, MEGA software was used to construct a Neighbor-joining (NJ) tree with 1000 bootstrapping based on the best model to assess the phylogenetic relationships within and among the study samples and reference samples.

Results

The mtDNA COI gene barcode sequences of 15 samples obtained during the analyses were compared with the database using the BLAST program and the species to which each of the samples belongs to were detected. As a result of the BLAST comparison, a total of 8 (eight) samples were revealed as Tilapia (*O. niloticus* and *O. mossambicus*) and 7 (seven) samples were revealed as Panga (*P. hypophthalmus*). The findings for each fillet are given in Table 1 below.

Table 1. Species detected by DNA barcode analysis of 15 fish fillet samples analyzed

Sample No	Species name on the package	Species name based on DNA barcoding analysis
1	*O. niloticus*	*O. niloticus*
2	*O. niloticus*	*O. niloticus*
3	*O. niloticus*	*O. mossambicus*
4	*O. niloticus*	*O. niloticus*
5	*O. niloticus*	*O. niloticus*
6	*O. niloticus*	*O. mossambicus*
7	*O. niloticus*	*O. niloticus*
8	*O. niloticus*	*O. mossambicus*
9	*O. niloticus*	*P. hypophthalmus*
10	*O. niloticus*	*P. hypophthalmus*
11	*O. niloticus*	*P. hypophthalmus*
12	*O. niloticus*	*P. hypophthalmus*
13	*O. niloticus*	*P. hypophthalmus*
14	*O. niloticus*	*P. hypophthalmus*
15	*O. niloticus*	*P. hypophthalmus*

The actual species names of the fish fillets revealed by the BLAST software were also prominent in the evolutionary relationship tree reconstructed by using MEGA 7 software (Figure 3).

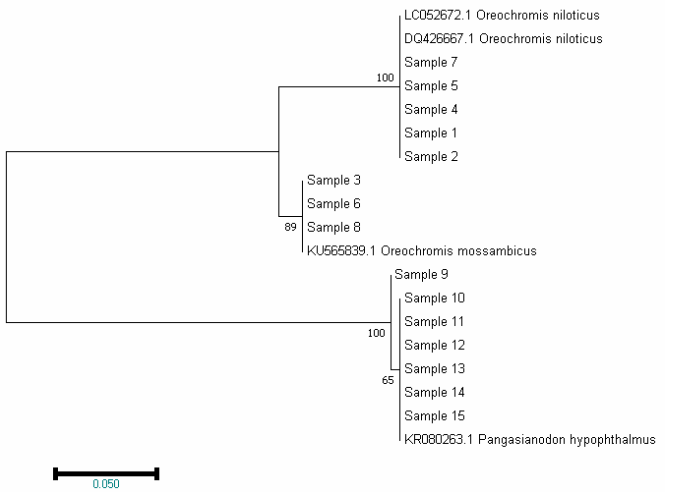

Figure 3. Phylogenetic relationship tree of the barcoding sequences of the 15 samples and the reference sequences, reconstructed by Neighbor-Joining method with 1000 bootstrap, based on HKY substitution model.

There were three clades revealed by phylogenetic tree. *P. hypophthalmus* reference sample and seven of the analyzed samples formed a distinct clade separating from Tilapia species (*O. niloticus* (Sample 1, 2, 4, 5, 7) and *O. mossambicus* (Sample 3, 6, 8)) with a 100% branch support. Moreover, reference samples from the two Tilapia species are divided into two different clades with high branch supports. The reference sample for *O. mossambicus* and three of the analyzed samples formed one clade with an 89% branch support and the reference samples for *O. niloticus* and five of the analyzed samples formed the other clade with a 100% branch support. These results were in consisted with the BLAST analysis.

Discussion

The studies around the world (e.g. the USA, Brazil, Italy, Iran, etc.) have reported to have a high rate of substitution in fish products (Barbuto et al., 2010; Filonzi et al., 2010; Changizi et al., 2013; Di Pinto et al., 2013, 2015; Staffen et al., 2017; Willette et al., 2017). For example, Neto (2013) has reported that in the labeling of seafood, tilapia is substituted by pangasius.

Understanding the incentive behind the mislabeling in fish products can be difficult to quantify because mislabelling may happen at any stage of the process. It may result from the fraud of the manufacturer, vendor, restaurateur or shop owner. However, it might also be resulted from the confusion of labeling laws, from misidentification based on morphological characters, or from using common vernacular. Being independent of the reason, what is often detected is that products of less value are substituted for more valuable fish suggesting an economic incentive for illegally substituting fish (e.g. Barbuto et al., 2010; Filonzi et al., 2010; Changizi et al., 2013; Di Pinto et al., 2013, 2015; Staffen et al., 2017; Willette et al., 2017).

In the present study, it was aimed at detecting whether the name of the species indicated on the frozen fish fillet packages was correct using DNA Barcoding technique. The BLAST analyses of the 15 DNA barcoding sequences obtained from the samples purchased from the shops have revealed that seven of them (47%) were indeed pangasius despite their label as being *O. niloticus*. Moreover, three of the eight tilapia fillets were of *O. mossambicus* origin; again, despite their labels as being *O. niloticus*. When a phylogenetic relationship tree was reconstructed including reference DNA barcoding sequences taken from NCBI (KU565839, DQ426667, LC052672, KR080263), the samples of the present study have grouped in three clades, as expected based on the BLAST search (Figure 3). In this phylogenetic tree, each clade included reference sequences of one of the three species: *O. niloticus*, *O. mossambicus* or *P. hypophthalmus*. These results provided evidence that commercial fraud and mislabelling can be observed in fillet fish products; one species substituting for another one as observed commonly across the world (Barbuto et al., 2010; Filonzi et al., 2010; Changizi et al., 2013; Di Pinto et al., 2013, 2015; Staffen et al., 2017). In this study, it was pangasius substituting for tilapia. Neto (2013) have proposed that substituting tilapia by pangasius is a marketing strategy to promote the consumption of these products. Furthermore, for the three of the samples, the genus name on the label was correct (*Oreochromis*), but not the species name (true species name is *O. mossambicus*).

There are few studies in Turkey reporting similar commercial fraud and mislabelling. In one of the studies, DNA barcoding analysis was carried out on surimi products sold in the markets, all of which were labeled as Alaskan Pollock (*Theragra chalcogramma*) on their packages (Keskin and Atar, 2012). Among these 50 surimi-based products, only 8 of them (%16) were found to be of Alaskan Pollock origin as declared on the product. Two of the samples were found to originate from different species and the rest of the samples were found to originate from different families like Sciaenidae, Synodontidae, Merlucciidae, Nemipteridae, etc. (Keskin and Atar, 2012). Another species identification study based on DNA barcoding analysis has been carried out on the 10 processed squid products purchased from the markets (Keskin and Atar, 2011). Among these, labels on the 6 of the squid products were reported as having lacked the information about the species origin of the products. The sequencing results revealed that the products were originated from 7 different species confined in two families: one is commercially high-valued Loliginidae family and the other one is commercially lower-valued Ommastrephidae family. Among the 10 samples, 4 of them were composed of the species belonging to the high-valued Loliginidae family and 6 of them were composed of the species belonging to the lower-valued Ommastrephidae family. Furthermore, they revealed that one of the four products informing the genus name on the label was mislabelled.

There are non-governmental organizations like Oceana (https://oceana.org) reporting fraud in seafood worldwide. One of the major concerns in such reports is that higher mercury levels detected in fraud fish products. Unfortunately, not all the countries, especially Asian countries, have the same chemical and handling regulations in aquaculturing fish. One might purchase a fish product thinking that he is buying a local high value fish, but instead it might turn out to be a substitute fish imported from Asia. Being uninformed/misinformed about what fish is on your plate may present a high health risk for you and your family in terms of heavy metal exposure or allergic reactions.

Conclusion

The increasing number of studies worldwide has proven that commercial fraud and mislabelling on aquatic food products and species substitutions are major problems in terms of food quality and food safety. Despite the conflicts caused by morphological identifications (especially for processed food), DNA barcoding analysis is a highly successful and applicable technique in seafood safety. The number of existing aquatic species is quite high such that the discrimination power of DNA barcoding was proven to be high, even for the identification of the local varieties (Galimberti et al., 2013). Strict monitoring based on DNA barcoding for end-to-end tracking supply chains and publicizing the results may help increased awareness in customers. Moreover, stricker regulations / laws on and increased consumer awareness may exert pressure on vendors to avoid fraud, which eventually would help decrease the rate of the fraud observed worldwide.

Conflict of Interest

The author declares that there is no conflict of interest.

References

Asensio, L., González, I., García, T. & Martín, R. (2008). Determination of food authenticity by enzyme-linked immunosorbent assay (ELISA). *Food Control*, ***19***: 1-8.

Barbuto, M., Galimberti, A., Ferri, E., Labra, M., Malandra, R., Galli, P. & Casiraghi, M. (2010). DNA barcoding reveals fraudulent substitutions in shark seafood products: the Italian case of Palombo (*Mustelus* spp.). *Food Research International*, ***43***: 376-381.

Bénard-Capelle, J., Guillonneau, V., Nouvian, C., Fournier, N., Le Loët, K. & Dettaï, A. (2015). Fish mislabelling in France: Substitution rates and retail types. *Peer J*, ***2***(9): e714.

Cawthorn, D-M., Steinman, H. A. & Witthuhn, R. C. (2012). DNA barcoding reveals a high incidence of fish species misrepresentation and substitution on the South African market. *Food Research International*, ***46***(1): 30–40.

Changizi, R., Farahmand, H., Soltani, M., Asarch, R. & Ghiasvand, Z., (2013). Species identification reveals mislabelling of important fish products in Iran by DNA barcoding. *Iranian Journal of Fisheries Sciences*, ***12***: 783–791.

Di Pinto, A., Di Pinto, P., Terio, V., Bozzo, G., Bonerba, E., Ceci, E. & Tantillo, G. (2013). DNA barcoding for detecting market substitution in salted cod fillets and battered cod chunks. *Food Chemistry,* ***141***: 1757–1762.

Di Pinto, A., Mottola, A., Marchetti, P., Bottaro, M., Terio, V.; Bozzo, G., Bonerba, E., Ceci, E. & Tantillo, G. (2015). Packaged frozen fishery products: Species identification, mislabelling occurrence and legislative implications. *Food Chemistry*, ***194***: 279–283.

FAO (2010). The State of World Fisheries and Aquaculture. (http://www.fao.org/3/a-i1820e.pdf) (Access date: 10.06.2019)

FAO (2017). Fishery and Aquaculture Statistics. Global production by production source 1950-2015 (Fishstat J). In: *FAO Fisheries and Aquaculture Department* [online]. Rome. (www.fao.org/fishery/statistics/software/fishstatj/en) (Access date: 15.06.2019).

FAO (2018a). *Overview of food fraud in the fisheries sector*, by Alan Reilly. Fisheries and Aquaculture Circular No. 1165. Rome, Italy.

FAO (2018b). The State of World Fisheries and Aquaculture. (http://www.fao.org/3/i9540en/i9540en.pdf) (Access date: 10.06.2019)

Filonzi, L., Chiesa, S., Vaghi, V. & Marzano, F. N. (2010). Molecular barcoding reveals mislabelling of commercial fish products in Italy. *Food Research International*, ***43***: 1383-1388.

Galimberti, A., Mattia, F. D., Losa, A., Bruni, I., Federici, S., Casiraghi, M., Martellos, S. & Labra, M. (2013). DNA barcoding as a new tool for food traceability. *Food Research International*, ***50***(1): 55-63.

Hasegawa, M., Kishino, H. & Yano, T. (1985). Dating of the human-ape splitting by a molecular clock of mitochondrial DNA. *Journal of Molecular Evolution,* ***22***(2): 160–174

Hebert, P. D. N., Cywinska, A., Ball, S. L. & de Waard, J. R. (2003). Biological identifications through DNA barcodes. *Proceedings of The Royal Society B: Biological Sciences,* ***270***(1512): 313-321.

Hubalkova Z., Kralik P., Tremlova, B. & Rencova, E. (2007). Methods of gadoid fish species identification in food and their economic impact in the Czech Republic: A review. *Veterinarni Medicina*, ***52***: 273-292.

Keskin, E. & Atar, H. H. (2011). İşlenmiş Kalamar Ürünlerinde Sitokrom Oksidaz I Gen Dizileri Kullanılarak Tür Tayini. *Gıda*, ***36***(6): 343-348.

Keskin, E. & Atar, H. H. (2012). Molecular identification of fish species from surimi-based products labelled as Alaskan pollock. *Journal of Applied Ichthyology*, ***28***: 811-814.

Kumar, S., Stecher, G. & Tamura, K. (2016) MEGA7: Molecular Evolutionary Genetics Analysis version 7.0 for bigger datasets. *Molecular Biology and Evolution*, ***33***(7): 1870-1874.

Maclean, J. (1984). Tilapia – The aquatic chicken. *ICLARM*, Makati, Manila. ***7***(1): 17.

Neto, D. A. P. (2013). Detec_cã de adultera_cão de espécies em pescado e derivados por meio detécnica de DNA Barcoding. Belo Horizonte (MG), Universidade Federal de MinasGerais, 43p. Available at http:// bibliotecadigital.ufmg.br

Özcan-Gökçek, E., Karahan, B. & Gamsız, K. (2012). Bir Nil Tilapya (*Oreochromis niloticus* L., 1758) populasyonunda BLUP yöntemiyle hasat ağırlığı için damızlık değer tahmini. *Ege Journal of Fisheries and Aquatic Sciences*, ***29***(1): 15-19.

Rehbein, H. (1990). Electrophoretic techniques for species identification of fishery products. *Zeitschrift für Lebensmittel-Untersuchung und Forschung*, ***191***(1): 1-10.

Smith, P. J., McVeagh, S. M. & Steinke, D. (2008). DNA barcoding for the identification of smoked fish products. *Journal of Fish Biology*, ***72*:** 464–471.

Staffen, C. F., Staffen, M. D., Becker, M. L., Löfgren, S. E., Muniz, Y. C. N., de Freitas R. H. A. & Marrero A. R. (2017). DNA barcoding reveals the mislabelling of fish in a popular tourist destination in Brazil. *Peer J*, ***5***: 1–13.

Strauss, R. E. & Bond, C. E. (1990). Taxonomic methods: morphology, pp 109-140. In: Schreck, C. B. & Moyle, P. B. (Eds.). Methods for fish biology. *American Fisheries Society*, Maryland. 704p.

TurkStat (2018). Turkish Statistical Institute. https://biruni.tuik.gov.tr/disticaretapp/menu.zul (Access date: 10.06.2019)

Ward, R. D., Zemlak, T. S., Innes, B. H., Last, P. R. & Hebert, P. D. (2005). DNA barcoding Australia's fish species. *Philosophical Transactions Royal Society B*, ***360***: 1847-1857.

Ward, R. D., Hanner, R. & Hebert, P. D. N. (2009). The campaign to DNA barcode all fishes. *Journal of Fish Biology*, ***74***(2): 329–356.

Willette, D. A., Simmonds, S. E., Cheng, S. H., Esteves, S., Kane, T. L., Nuetzel, H., Pilaud, N., Rachmawati, R. & Barber, P. H. (2017). Using DNA barcoding to track seafood mislabeling in Los Angeles restaurants. *Conservation Biology*, ***31***(5): 1076-1085.

World Bank (2013). *FISH TO 2030. Prospects for Fisheries and Aquaculture.* World Bank Report Number 83177-GLB. (http://www.fao.org/3/i3640e/i3640e.pdf) (Access date: 28.06.2019)